

**Implementation and Justification of Innovated Three Lines Loop for  
Single and Multi- Phase Flows Studies**

by

Cheah Zi Chian

16632

Dissertation submitted in partial fulfilment of  
the requirements for the  
Bachelor of Engineering (Hons)  
(Mechanical)

JANUARY 2016

Universiti Teknologi PETRONAS  
Bandar Seri Iskandar  
31750 Tronoh  
Perak Darul Ridzuan

CERTIFICATION OF APPROVAL

**Implementation and Justification of Innovated Three Lines Loop for  
Single and Multi- Phase Flows Studies**

by

Cheah Zi Chian

16632

A project dissertation submitted to the  
Mechanical Engineering Programme  
Universiti Teknologi PETRONAS  
in partial fulfilment of the requirements for the  
Bachelor of Engineering (Hons)  
(MECHANICAL)

Approved by,

---

(PROFESSOR DR. HUSSAIN AL-KAYIEM)

UNIVERSITI TEKNOLOGI PETRONAS  
TRONOH PERAK  
January 2016

## CERTIFICATION OF ORIGINALITY

This is to certify that I am responsible for the work submitted in this project, that the original work is my own except as specified in the references and acknowledgements, and that the original work contained herein have not been undertaken or done by unspecified sources or persons.

---

CHEAH ZI CHIAN

## ABSTRACT

In Mechanical Engineering Department of Universiti Teknologi PETRONAS (UTP), there are plenty of ongoing as well as future research studies on various directions on fluid flow. Hence, this raises the need of building many categories of flow lines. However, it incurred high cost, space and required man power for this. Hence, in the present work, the innovated three lines flow loop was designed, fabricated and justified. The experimental flow loop or sometimes known as test rig or test loop, can be used to generate experimental results or for validation with numerical simulation in research studies.

During the design stage, the required specifications of the flow loop was studied and planned. The three lines flow loop system was constructed successfully according to the requirements. The measuring and control unit in the system including centrifugal pump, solenoid valve, liquid mass flow meter, air flow meter and online computer control unit (data acquisition system). On the other hand, the justification of flow loop system was done based on the head losses in the system. The theoretical calculated head losses values,  $\Sigma h_{L,cal}$  were determined based on Darcy-Weisbach equation whereas experimental head losses value,  $\Sigma h_{L,exp}$  were measured by recording the pressure drop and elevation changes. The results exhibited good relationship between  $\Sigma h_{L,exp}$  and  $\Sigma h_{L,cal}$  at varying flow rates as they fall in the percentage error range of 6-25% of error.. The differences between  $\Sigma h_{L,exp}$  and  $\Sigma h_{L,cal}$  can be improved by installing more sensitive pressure gauge and further investigate on the loss coefficient of pipe fittings in future.

It is expected that such three lines flow loop system will be able to conduct multiple experiments in fluid flow directions in the future and therefore lead to significant research benefits.

## ACKNOWLEDGEMENTS

First and foremost, the author would like to express the very great appreciation to the UTP for offering final year students to conduct a 28 weeks Final Year Project (FYP). It is indeed a golden opportunity for students to experience in research and development and develop technical and communication skills through all the activities and tasks involved.

Besides that, the author also would like to extend utmost gratitude to the direct supervisor, Professor Dr. Hussain Al-Kayiem for all the time and effort he has spent and contributed. He patiently guides and advises the author on conduction of experiment, report writing and preparation for presentation. Under his supervision, the author able to improve the quality of project.

Furthermore, the author would like to express the special thanks to co-supervisor, Dr. Dereje Woldemichael. His continuous assistance and motivations help the author in completing the project. Besides that, the author would like to address thank you to my colleagues Azri, Harrison, Lee Wen Ching, Derek Ho, Farbod, Nafif and Faidhi. The author appreciates very much from their kind support. Plus, the author is enlightened by their experiences and brilliant ideas and from that; the author is certainly benefited in technical skills.

Other than them, the author also would like to thank UTP Research Innovation Office (RIO) on giving approval for purchasing all the materials in order to build the test rig.

## TABLE OF CONTENTS

<b>ABSTRACT .....</b>	<b>iii</b>
<b>ACKNOWLEDGEMENTS .....</b>	<b>iv</b>
<b>LIST OF FIGURES.....</b>	<b>vi</b>
<b>LIST OF TABLES.....</b>	<b>vii</b>
<b>NOMENCLATURES .....</b>	<b>viii</b>
<b>CHAPTER 1 INTRODUCTION.....</b>	<b>1</b>
1.1 Background .....	1
1.2 Problem Statement.....	3
1.3 Objectives .....	3
1.4 Scope of Study .....	3
<b>CHAPTER 2 LITERATURE REVIEW .....</b>	<b>4</b>
2.1 Fluid Storage and Supply.....	5
2.2 Measurement and Control Devices.....	6
2.3 Test Loop .....	8
2.4 Summary on Literature Review .....	8
<b>CHAPTER 3 METHODOLOGY/PROJECT WORK.....</b>	<b>10</b>
3.1 Project Flow Chart .....	10
3.2 Project Activities.....	12
3.2.1 Design and Implementation of Three Lines Flow Loop .....	12
3.2.2 Experimental Justification on the Three Lines Flow Loop System .....	13
3.3 Project Timeline (Gantt Chart) .....	17
3.4 Key Milestones .....	18
<b>CHAPTER 4 RESULTS AND DISCUSSION .....</b>	<b>19</b>
4.1 Design and Implementation of Three Lines Flow Loop System .....	19
4.1.1 2inch, 3inch and 4inch Flow Line .....	25
4.1.2 Installation of Pressure Gauge.....	28
4.2 Justification on Three Lines Flow Loop System .....	29
4.2.1 Experimental Values of Head Losses .....	29
4.2.2 Theoretical Head Losses Calculations.....	30
4.2.3 Comparison between Experimental and Theoretically Calculated Values of Head Losses .....	33
<b>CHAPTER 5 CONCLUSION AND RECOMMENDATION .....</b>	<b>36</b>
<b>REFERENCE .....</b>	<b>37</b>
<b>APPENDIX .....</b>	<b>39</b>

## LIST OF FIGURES

Figure 1: Schematic of flow loop built by Tang et. al [3].	2
Figure 2: Schematic diagram of batch fluidized bed reactor [7].	2
Figure 3: Closed flow loop which developed by Kee et al. [8].	4
Figure 4: An opened flow loop that built for study windowless spallation zone flow pattern by Xiong et al. [4].	5
Figure 5: Project flow chart.	11
Figure 6 Gantt Chart.	17
Figure 7: Key milestone of project for both FYP 1 and FYP 2.	18
Figure 8: Schematic diagram of integrated three lines flow loop.	21
Figure 9: The inlet section of the flow loop, the storage tank, pump, solenoid valve and mass flow meter.	22
Figure 10: The connection of the flow loop at the inlet where the flow branched into three lines.	22
Figure 11: From the left, 3inch, 2inch and 4inch flow line, each flow line has total length of 24m.	23
Figure 12: Steel support stand for pipe.	23
Figure 13: Receiver tanks connection.	24
Figure 14: The pump was anchored to ground and a rubber pad was beneath the pump to absorb vibration.	24
Figure 15: 2inch flow line.	26
Figure 16: 3inch flow line.	26
Figure 17: 4inch flow line with 0 degree inclination.	27
Figure 18: 4inch flow line with 45 degree inclination.	27
Figure 19: 4inch flow line with 90 degree inclination.	27
Figure 20: $\Sigma hL$ against Q in 2inch flow line.	34
Figure 21: $\Sigma hL$ against Q in 3inch flow line.	34
Figure 22: Percentage error on $\Sigma hL$ for 2inch flow line.	35
Figure 23: Percentage error on $\Sigma hL$ for 3inch flow line.	35

## LIST OF TABLES

Table 1: Fluid supply devices.....	6
Table 2: Measurement and control devices that applied in corresponding research studies.....	6
Table 3: Test loop details from past experiments.....	9
Table 4: Fluid flow general characteristics. ....	12
Table 5: Surface roughness coefficient for some common pipe materials.....	16
Table 6: List of component that used in the integrated three lines flow loop. ....	20
Table 7: Calculation on entrance length of respective flow line. ....	28
Table 8: Q, v, P and z readings at the inlet and outlet and computed $\Sigma hL, exp$ for 2inch flow line.....	30
Table 9: Q, v, P and z readings at the inlet and outlet and computed $\Sigma hL, exp$ for 3inch flow line.....	30
Table 10: Length of the loop, diameter of pipe and loss coefficient, $\Sigma K L$ for 2inch loop.....	31
Table 11: Recorded, Q and computed v, Re, f, $hL, major$ , , $hL, minor$ and , $\Sigma hL, cal$ for 2inch loop.....	31
Table 12: Length of the loop, diameter of pipe and loss coefficient, $\Sigma K L$ for 3inch supply and test sections. ....	32
Table 13: Recorded, Q and computed v, Re, f, $hL, major$ , , $hL, minor$ and , $\Sigma hL, cal$ for 3inch loop.....	32



## NOMENCLATURES

$A$	Cross-section area
$h_{L,major}$	Major losses
$h_{L,minor}$	Minor losses
$K_L$	Loss coefficient of fittings
$L$	Length
$P$	Pressure
$Q$	Flow rate
$Re$	Reynold number
$v$	Velocity
$z$	Elevation
$\Sigma h_{L,cal}$	Theoretically calculated total head losses
$\Sigma h_{L,exp}$	Experimentally computed total head losses
$\Sigma K_L$	Total loss coefficient

# CHAPTER 1

## INTRODUCTION

In this chapter, the background study describes on utilities of flow loop in research investigations and some different categories of flow loop which done by other researchers are briefly described. The problem statement, objectives and scope of study are defined as well in this chapter.

### 1.1 Background

The experimental flow loop or sometimes known as test rig or test loop, is regarded as well-founded research methodology. It can be used for multiple purposes such as study on the desired parameters in a flow loop, validation of the expected or estimated results with numerical simulation and testing the feasibility of the designed prototype. There are many categories of flow loop which can be used for different disciplines of studies such as thermodynamic, nuclear engineering, biomass, and fluid mechanics.

Abed et al.'s [1] and Qu et al.'s [2] flow loop are thermodynamic-related where the laminar flow characteristics, forced convection heat transfer, pressure drop and heat transfer characteristics were studied in the experiments. Meanwhile, Tang et al. [3] had compared the results of numerical simulation of turbulent flow characteristics and heat transfer performances with analytical solution. Figure 1 shows the flow facility built by Tang and the team.

A nuclear reactor was developed by Xiong et al. [4] to study the windowless spallation zone flow pattern. On the other hand, batch fluidized-bed reactor and continuous reactor were used to conduct experiments on biomass gasification using chemical looping (BGCL) [5]. Figure 2 shows the schematic diagram of batch fluidized bed reactor.

In order to assess the designed prototype which supposed to have the ability of measure multiphase flow rate and display the image of flow distribution, therefore the prototypes were being tested in fluid flow loops for validation [6,7].

All of these show vast significances on having flow loop in research studies career. The focus of this project is design and fabrication of innovated three line loops which can be applied for both single and multi- phase flows.

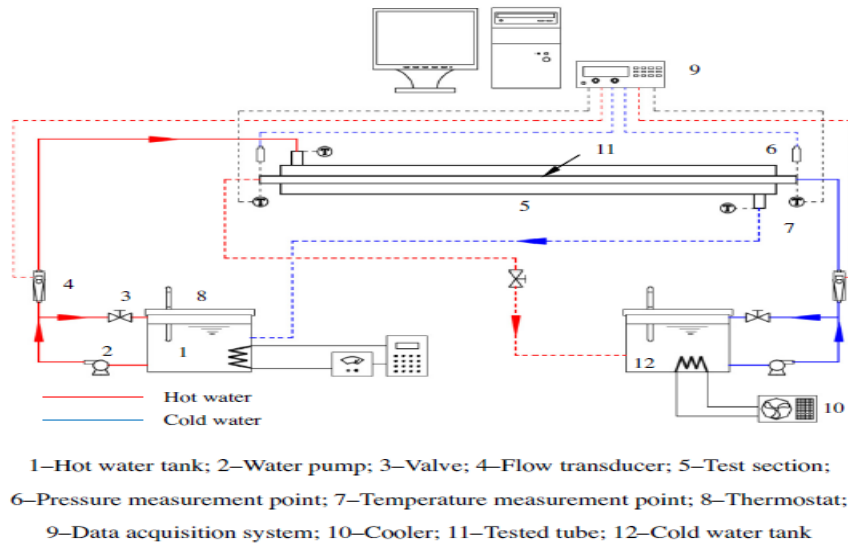


Figure 1: Schematic of flow loop built by Tang et. al [3].

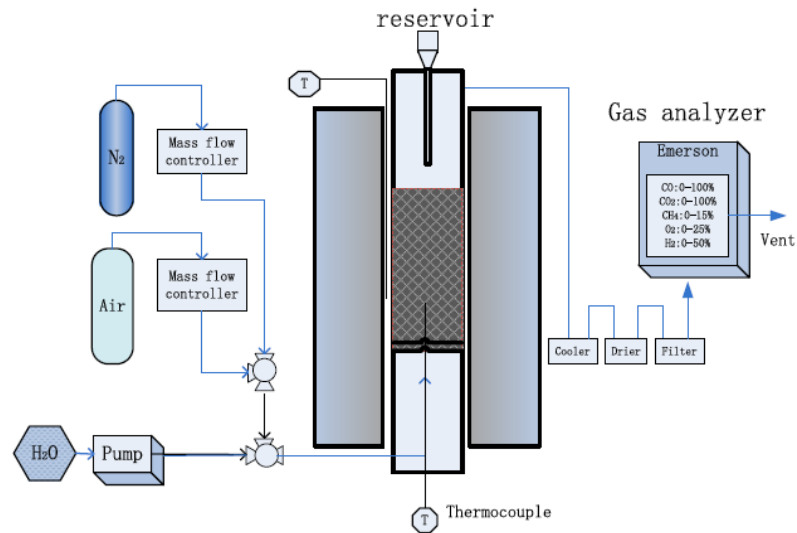


Figure 2: Schematic diagram of batch fluidized bed reactor [7].

## 1.2 Problem Statement

In Mechanical Engineering Department, Universiti Teknologi PETRONAS (UTP), there are plenty of ongoing research studies on fluid flow from different directions, for instance invented smart pig for pipe cleaning in single phase flow, studies on slug flow fluid structure interaction, two-phases flow for T-junction stand pipe separator and etc. These raise the need of building many categories of flow lines in order to validate the numerical solutions with experimental simulation. However, installation of all types of the flow loops will incur high investment of cost and require definite space. Hence, developing an integrated three line flow loops will be able to meet the research project requirements and at the same time optimize cost, space and effort.

## 1.3 Objectives

The main objectives of this project are to:

- i. To design and implement innovated three line flow loop.
- ii. To experimentally investigate and justify 2inch and 3inch flow lines of the flow loop

## 1.4 Scope of Study

The identified scope of study are:

- i. Fabrication of 2, 3, and 4 inch inner diameter flow lines with total length of 24m for each line.
- ii. Compute experimental head losses,  $\Sigma h_{L,exp}$  and calculate theoretically on the head losses,  $\Sigma h_{L,cal}$  for 2inch and 3inch flow lines.
- iii. Justify and validate the experimental flow loop by comparing the theoretical calculation and experimental computation for 2inch and 3inch flow lines.

## CHAPTER 2

### LITERATURE REVIEW

Some studies on other researchers' flow loop are done and the information is recorded accordingly. There are two type of flow loop, namely closed flow loop and opened flow loop. A closed flow loop is designed in such a way that to recycle the fluid flow in the system whereas an opened flow loop is developed to discharge the fluid out from the experimental setup. Most of the experiments were constructed in closed flow loop manner because it is more cost-effective and sustainable test rig. Figure 3 shows an example of closed loop which developed by Kee et al. [8] while Figure 4 shows an opened flow loop that built for study windowless spallation zone flow pattern by Xiong et al. [4].

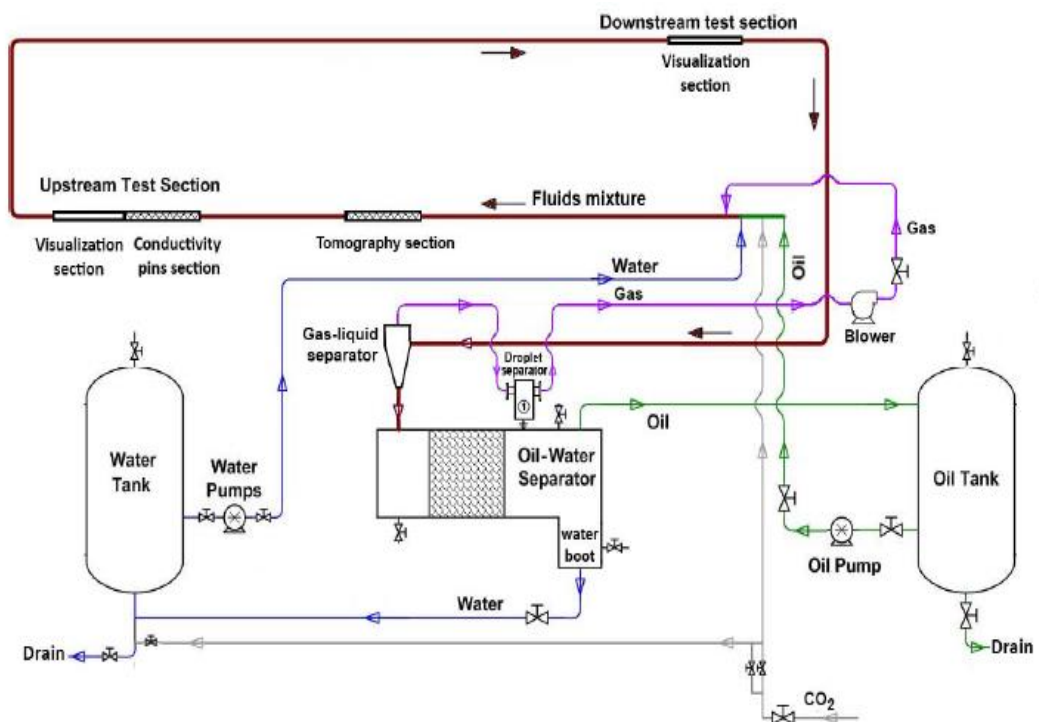


Figure 3: Closed flow loop which developed by Kee et al. [8].

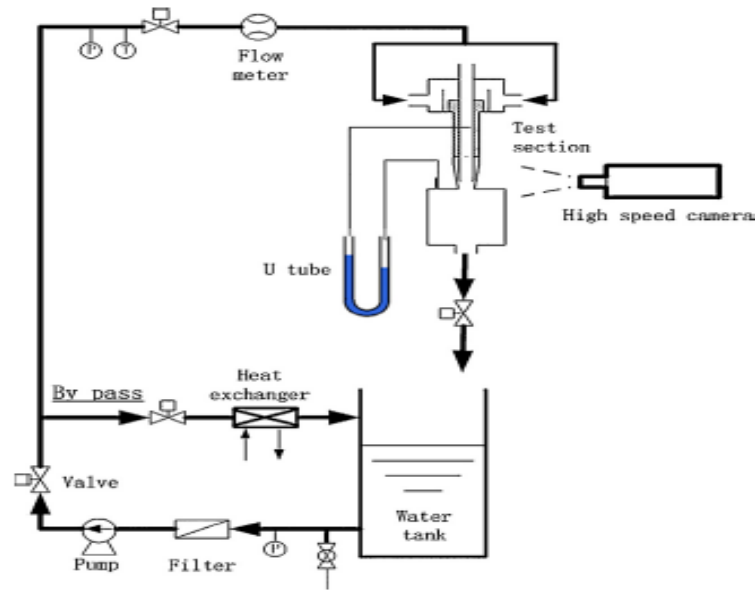


Figure 4: An opened flow loop that built for study windowless spallation zone flow pattern by Xiong et al. [4].

In general, flow loop is divided into five main sections, namely fluid storage and supply, measurement and control devices and test loop.

## 2.1 Fluid Storage and Supply

The common fluids that used in a flow loop include water, oil and air. The liquid is stored in storage tank or reservoir whereas the air is normally supplied by air compressor [1-3,6,8-13]. In Abdullah et al.'s [12] experiment, water was stored in 100 gallon capacity as supply tank which the water was to be fed into the test loop whereas additional 80 gallon water tank was connected with the supply tank and acted as receiver tank, to collect water at the outlet of the loop. By using this tank connection configuration, debris and air bubbles at the inlet of pump can be avoided. On the other hand, Wu et al. [13] had used stainless steel slurry tank which has volume of  $1\text{ m}^3$  to store slurry and keep it at homogenous state. In Li et al.'s [10] and

Ye et al.'s [11] experiments, the air is compressed into buffer vessel to reduce the pressure fluctuation. It is common to known that pump is used to supply and force liquid into flow loop; meanwhile the air is compressed [2,8-12]. Table 1 below shows the summary of fluid types and fluid supply devices by each author in their respective experiments.

Table 1: Fluid supply devices.

Author	Type of Fluids	Fluid Supply Devices
Qu et al. [2]	Water	Gear pump
Kee et al. [8]	Water, oil	Progressive cavity pump
	Air	Positive-displacement type gas blower
Lv et al. [9]	Water, oil	Custom-made magnetic pump
	Air	Plunger compressor
Li et al. [10]& Ye et al. [11]	Water, oil	Centrifugal pump
	Air	Screw compressor by maintain the pressure at 0.8MPa
Abdullah et al. [12]	Water	(EBARA 3M 50-125/2.2) pump with maximum flow rate of $1 \text{ m}^3 \text{ s}^{-1}$ and head of 19m.
	Air	Central compressor (Ingersoll rand) which delivered maximum air of $42.5 \text{ m}^3 \text{ min}^{-1}$ at pressure up to 0.85 MPa
Wu et al. [13]	Slurry	Centrifugal pump which supply $80 \text{ m}^3$ slurry per unit hour and 12 MPa pumping pressure at the maximum power

## 2.2 Measurement and Control Devices

The basic instrumentation in a test facility includes flow meter, pressure sensor, temperature sensor, and high speed camera. Table 2 tabulates the measurement and control devices that applied in corresponding experiments.

Table 2: Measurement and control devices that applied in corresponding research studies.

Author	Measurement and Control Devices	Descriptions
Xiong et al. [4]	Electric magnetic flow meter	Measure liquid flow rate with accuracy of 0.5%.
	U-tube	Measure pressure difference with error of 10 Pa.
	Pressure transmitter	Measure pressure with accuracy of $\pm 0.1\%$
	T- type thermocouple	Regulate the temperature with accuracy of $\pm 0.5 \text{ }^\circ\text{C}$ .
	Phantom V310 high speed camera	Record the visualization of flow pattern.
Ge et al. [5]	K-type thermocouple	Control reaction temperature
	NGA2000 type gas analyzer	A type of gas analyzer from EMERSON Company, USA, use to measure composition of gaseous product.

<b>Kee et al. [8]</b>	Vision Research Phantom V12.1 high speed camera	Capture the fast-motion multiphase fluid flow patterns.
<b>Lv et al. [9]</b>	Coriolis flowmeter	Measure the multiphase liquid density and flow rate which has the range from 0 to 3600 kg/h.
	Differential-pressure sensors	Measure the differential pressure with accuracy of 0.05%.
	Piezo- resistive pressure transducers	Has accuracy of 0.1%.
	FM1000 $\gamma$ -ray densitometers	Measure the mean density of the multiphase fluid.
	Focused beam reflectance measurement (FBRM) probe and a particle video microscope (PVM) probe	Use to visualize if any object droplets, bubbles, and solid particles carried inside the flow at the inlet of test section.
<b>Li et al. [10]&amp; Ye et al. [11]</b>	Orifice system	Measure air flow rate by using 3 regulating valves.
	Electromagnetic flow meters	Measure the liquid (water and oil) flow rate with accuracy of 0.5%.
	Mass flow meters	Measure liquid mass flow rate with accuracy of 0.1%.
	Thermocouples	Installed before flow meters and use to regulate the flow temperature
<b>Abdullah et al. [12]</b>	Centrifugal Pump (EBARA 3M 50-125/2.2)	
	Mass flow controller (Omega FMA-2600A)	Measure and regulate the air flow rate within the range from 0-2 $Sm^3min^{-1}$ with accuracy of $\pm 0.05\%$ .
	Phantom 9.2 high speed video camera	Capable to record up to three million frames per second, able to determine the slug velocity
<b>Wu et al. [13]</b>	Electromagnetic flow meter	Measure slurry volumetric flow rate
	Sampling probe	Measure the concentration of slurry
	Differential pressure transducer	Collect the partial and total pressure drop values.



### **2.3 Test Loop**

Pipeline is the main medium that uses to transport the fluid in a test loop. The selection of pipeline material selection is very important; it must be strong enough to sustain the pressure and heat. The test section in a flow loop normally is built with transparent material, so that it is visible for observation. There are a few configuration of flow loop e.g. horizontal, vertical, inclined, riser-like or combination of these [8-13]. The flow loop is designed based on the purposes of conducting the research. Table 3 shows the test loop details which had done in the previous researches.

### **2.4 Summary on Literature Review**

In short there are various choice on selecting fluid storage and supply, types of measurement and control devices as well as test loop materials and length. Each of them having different specifications and functions depending on design. Hence, engineering judgements and reasoning shall be applied while designing the flow loop system. Cost consideration shall be emphasized too.

Table 3: Test loop details from past experiments.

Author	Test Sections	Descriptions
<b>Kee et al. [8]</b>	Main flow loop	30m long PVC flow line with 0.1m inner diameter was built and mounted on steel rig structure. The loop has inclined capability which from 0° (horizontal) to 90° (vertical). Transparent PVC pipe was used in the loop as well for visualization purpose.
<b>Lv et al. [9]</b>	Main flow loop	There are 2 different sizes of pipe joined together to form a 30m stainless steel flow loop. One of the pipe has inner diameter of 2.54cm (1in) whereas another has inner diameter of 5.00mm (2in).
<b>Li et al. [10]&amp; Ye et al. [11]</b>	Horizontal pipeline	114m long horizontal stainless steel pipe was built to ensure fully developed flow.
	Downward inclined section	In order to stabilize the pipeline flow regime before entry into the riser and provides appropriate gas compressible volumes for the beginning of severe slugging, a length of 16m pipeline was constructed. The selected pipeline materials is stainless steel.
	Riser-like pipeline	The lazy S-shaped riser is made up of 3 sections which are 15.3m vertical height when downward inclination at -2°, 13.1m upper limb, 6.2m lower limb and 4.0m downcomer of riser. This test section is made up of transparent plastic flexible tube for observation usage. A 50mm inner diameter choke was included at the riser top.
<b>Abdullah et al. [12]</b>	Main flow loop	An 8m long pipeline made up from Plexiglas are built on a fixed steel structure which mount to the ground, to reduce the vibration effect. The inner diameter of the main flow loop is 0.074m.
<b>Wu et al. [13]</b>	Main flow loop	The built flow loop has total length of 35m with inner diameter of 120 mm.

## **CHAPTER 3**

### **METHODOLOGY/PROJECT WORK**

The main focus of this project is to integrate three different sizes of diameter flow lines (particularly 2inch, 3inch and 4inch) into one closed system in Advanced Fluid Dynamics Lab (17-01-10), Universiti Teknologi PETRONAS. This project covered design, implementation as well as justification of the flow loops. The justification of the flow loops was investigated by comparing the differential pressure with the calculated differential pressure. Project flow chart was planned to develop understanding of how a process was done; meanwhile Gantt chart illustrates the entire project schedule.

#### **3.1 Project Flow Chart**

A systematic approach was used to run the project. Figure 5 shows the project flow chart.

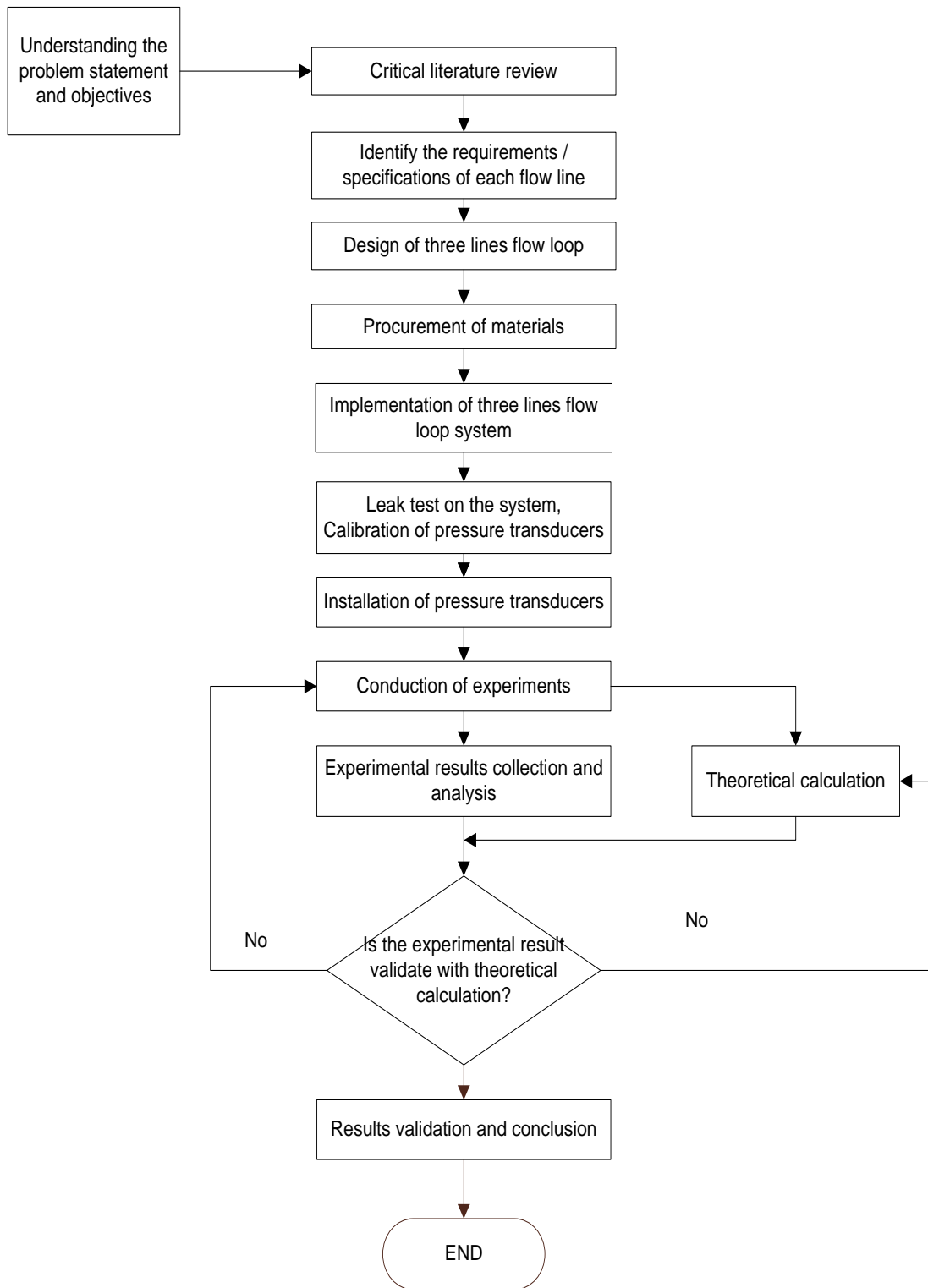


Figure 5: Project flow chart.

## 3.2 Project Activities

After understanding the project objectives and identified the scopes of study, the main project activities are design and implementation of three line flow loop system as well as experimental justification on the system by using calculation approach.

### 3.2.1 Design and Implementation of Three Lines Flow Loop

The three lines flow loop actually stand for 2in, 3in and 4in diameter of pipeline. Before designing the three lines flow loop, the purposes of requiring of 2in, 3in and 4in flow loop were studied. The schematic diagram of the flow loop system is as shown in Figure 8 (Chapter 4, under the section of 4.1) and is further discussed in Chapter 4.

In order to enhance the performance and accuracy of pressure gauge in the experiment, the pressure gauges that measure inlet of the three flow lines are installed after the entrance length of respective flow lines. This is because after the entrance length, the flow is fully developed. The entrance lengths were calculated based on general characteristics of pipe flow which are laminar, transition and turbulent flow [14,15]. Table 4 shows the condition of fluid flow characteristics.

Table 4: Fluid flow general characteristics.

Flow Characteristics	Re
Laminar Flow	$Re < 2100$
Transition Flow	$2100 < Re < 4000$
Turbulent Flow	$Re > 4000$

Re is the Reynold number and is computed by:

$$Re = \frac{\rho v D}{\mu} \quad \text{Eq. 1}$$

Where,

$\rho$ : density of the fluid ( $kg/m^3$ )

$v$ : fluid velocity ( $m/s$ )

$D$ : diameter of the flow stream ( $m$ )

$\mu$ : dynamic viscosity of fluid ( $Ns/m^2$ )

The entrance length was calculated based on:

$$\text{Laminar Flow: } l_e = 0.06 Re * D \quad \text{Eq. 2}$$

$$\text{Turbulent Flow: } l_e = 4.4 D * Re^{\frac{1}{6}} \quad \text{Eq. 3}$$

The implementation of three lines flow loop includes purchasing the necessary materials, pipe fittings, glue, support stand as well as assemble them into a functioning system.

### 3.2.2 Experimental Justification on the Three Lines Flow Loop System

Justification on the three lines flow loop system was done by comparing the percentage error of head losses,  $\Sigma h_L$  in the actual flow loop with the theoretical calculations by using Darchy-Weisbach equation.

Firstly, the experimental head losses values,  $\Sigma h_{L,exp}$  were computed by using derived energy equation as shown in Eq. 4. Since there are two pressure gauges installed at the inlet and outlet of each of the three flow lines, therefore the  $P_1$  and  $P_2$  values can be measured experimentally. Meanwhile, the velocity,  $v$  at the inlet and outlet can be computed by using Eq. 5, where the flow rate,  $Q$  can be read from flow meter and the cross-section area,  $A$  of the pipe can be determined by using Eq. 6. If there is change in  $A$  in any of the flow line, the velocity can be computed by using Eq. 7 which follow the conservation of flow rate in a closed system. The elevation of the 2 points,  $z_1$  and  $z_2$  can be measured experimentally by defining a reference line.

$$\Sigma h_{L,exp} = \frac{(P_1 - P_2)}{\gamma} + \frac{(v_1 - v_2)}{2g} + (z_1 - z_2) \quad \text{Eq. 4}$$

$$v = \frac{Q}{A} \quad \text{Eq. 5}$$

$$A = \frac{\pi}{4} D^2 \quad \text{Eq. 6}$$

$$v_2 = \frac{A_1 v_1}{A_2} \quad \text{Eq. 7}$$

On the other hand, Darchy-Weisbach equation was used to determine the calculated differential pressure,  $\Sigma h_{L,exp}$  [14,15]. However, there are some limitations (assumptions) for this equation, which are:

- i. The fluid is incompressible
- ii. There is no energy loss in the fluid flow.

Typically in fluid flow analysis, the pressure loss are referred to “head”. According to Darcy’s equation, head loss,  $\Sigma h_L$  is defined as the total energy loss in the system, and it is the summation of major loss,  $h_{L,major}$  and minor loss,  $h_{L,minor}$ .

$$\Sigma h_{L,cal} = h_{L,major} + h_{L,minor} \quad \text{Eq. 8}$$

$h_{L,major}$  is due to friction in the pipe wall and friction between the pipe wall and fluid flowing through it (viscosity of the fluid).  $h_{L,major}$  is proportional to the velocity head of the flow and ratio of the length to the diameter of the flow stream. The  $h_{L,major}$  can be evaluated by using Eq. 9.

$$h_{L,major} = f \times \frac{L}{D} \times \frac{v^2}{2g} \quad \text{Eq. 9}$$

Where,

$L$ : length of the flow stream (m)

$D$ : diameter of the flow stream (m)

$v$ : fluid velocity (m/s)

$f$ : dimensionless friction factor

$f$  is a dimensionless friction factor and is determined based on the general characteristics of the flow. If the flow is laminar, then  $f$  is calculated by using Eq. 10.

$$f = \frac{64}{Re} \quad \text{Eq. 10}$$

If the flow is turbulent, then  $f$  is determined by using Colebrook Equation or Moody Chart. Moody Chart gives the functional dependence of  $f$  on  $Re$  and  $\varepsilon/D$  [14,15]. Refer to Appendix 1 for Moody Chart. Colebrook Equation is as shown as below and it was used to calculate friction factor in this project.

$$f = \frac{0.25}{\left[\log\left(\frac{1}{3.7\left(\frac{D}{\epsilon}\right)} + \frac{5.74}{Re^{0.9}}\right)\right]^2} \quad \text{Eq. 11}$$

$\epsilon$  is the surface roughness of duct or pipe flow and it is depends on the materials of the conduit. Table 5 shows the surface roughness for some common pipe materials [16].

Unavoidably, in every flow system must consists of pipe fittings and control devices e.g. valve, socket joint, tee joint, flow meter and etc. These add to the overall head loss system and is termed as minor loss,  $h_{L,minor}$ . The  $h_{L,minor}$  is calculated by using the formula:

$$h_{L,minor} = \Sigma K_L \times \frac{v^2}{2g} \quad \text{Eq. 12}$$

The loss coefficient,  $K_L$  is a dimensionless parameter and strongly dependent on the geometry of the component and  $v$ . It is also vary depending on the size and material of the component. Refer to Appendix 1 for the values of  $K_L$  base on geometry and situation [14,17].

The relationship between  $\Sigma h_{L,exp.}$  and  $\Sigma h_{L,cal.}$  against  $Q$  will be studied and displayed in Chapter 4 after obtaining the results. The percentage error between  $\Sigma h_{L,exp.}$  and  $\Sigma h_{L,cal.}$  is calculated by using Eq. 13 and the percentage error shall be as low as below 35%.

$$\frac{\Sigma h_{L,exp.} - \Sigma h_{L,cal.}}{\Sigma h_{L,exp.}} \times 100\% \quad \text{Eq. 13}$$



Table 5: Surface roughness coefficient for some common pipe materials.

Surface	$\epsilon$ (m) $10^{-3}$
Copper, Lead, Brass, Aluminum (new)	0.001 - 0.002
PVC and Plastic Pipes	0.0015 - 0.007
Stainless steel	0.015
Steel commercial pipe	0.045 - 0.09
Stretched steel	0.015
Weld steel	0.045
Galvanized steel	0.15
Rusted steel (corrosion)	0.15 - 4
New cast iron	0.25 - 0.8
Worn cast iron	0.8 - 1.5
Rusty cast iron	1.5 - 2.5
Sheet or asphalted cast iron	0.01 - 0.015
Smoothed cement	0.3
Ordinary concrete	0.3 - 1
Coarse concrete	0.3 - 5
Well planed wood	0.18 - 0,9
Ordinary wood	5

### 3.3 Project Timeline (Gantt Chart)

The Gantt chart is developed base on 28 weeks timeline and use to plan, monitor and coordinate the progress of the project. Figure 6 shows the Gantt chart for both Final Year Project (FYP) 1 and FYP 2.

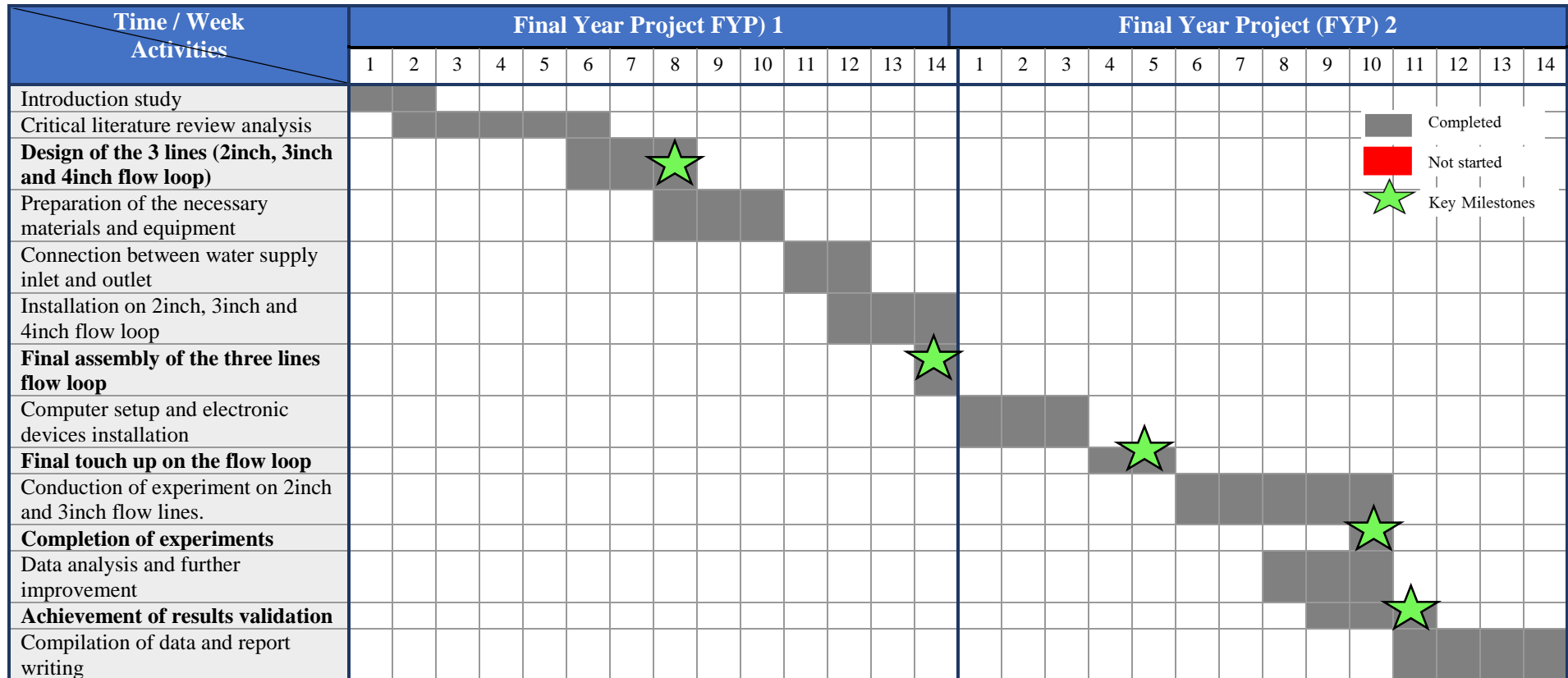


Figure 6 Gantt Chart.

### 3.4 Key Milestones

There are four key milestones identified in this project as shown in the Gantt chart (refer to Figure 6). Figure 7 further explains on the expected the progress according to the timeline.

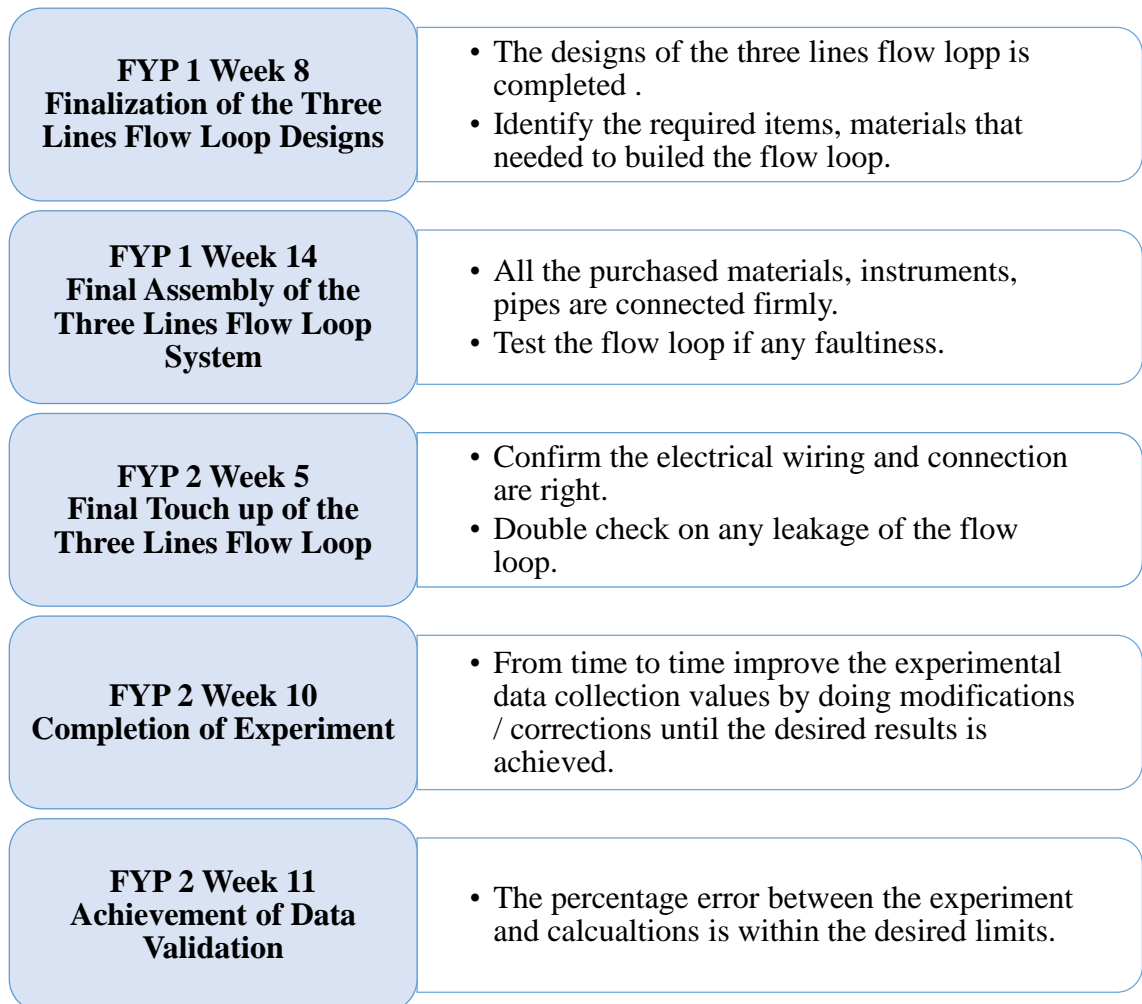


Figure 7: Key milestone of project for both FYP 1 and FYP 2.

## CHAPTER 4

### RESULTS AND DISCUSSION

In this chapter, the design and implementation of three lines flow loop system are described and the justification of flow loop system is presented.

#### 4.1 Design and Implementation of Three Lines Flow Loop System

The schematic diagram of integrated three lines flow loop is as shown in Figure 8. Figure 9-12 show the three line flow loop test rig setup.

Three water tanks were used in the flow loop, the supply tank has the volume of 100 gallon whereas each of the two receiver tanks has capacity of  $0.2m^3$ . Since the 3inch flow line carry two-phase flow (water and air), therefore the two receiver tanks serve as buffer tanks to let the air escape to the atmosphere. Besides that, the receiver tanks avoid the water outlet directly flow into supply tank, thus the centrifugal pump is protected from damages by air cavitation. Figure 13 shows the connection of receiver tanks.

Since the pump having high flow rate, therefore the pump was anchored to the floor by using wall plug for safety purpose. In addition, rubber pad was placed beneath the pump to absorb vibration from the pump as shown in Figure 14. A solenoid valve was installed right after the pump, to enable the users to control the flow rate of pump. On the other hand, the air flow meter was installed after the gas compressor. These three devices were then connected in a computer controller and the software namely Test Rig System. This software allows the users to control the flow rate of pump as well as getting the reading of air flow meter. Apart from that, FLT Liquid Turbine Flow Meter was installed after the solenoid valve to measure the water flow rate. Besides that, there are also pressure gauges installed on the 2inch and 3inch flow lines.

This flow loop system was designed in such a way that, only one of flow lines can be activated at one time. The ball valve at the inlet of each flow line is used to block

the water from flowing into the loop; so that during the operation, one flow line is running whereas the other two flow lines are isolated.

Table 6 list the measurement and control devices that used in the integrated three lines flow loop.

Table 6: List of component that used in the integrated three lines flow loop.

Measurement and Control Device	Description	
<b>Centrifugal Pump</b>	Model	EBARA 3M 50-125/2.2
	Flow rate range	24 to 60 $m^3 h^{-1}$
	Head range	8 to 19m
<b>Liquid Flow Meter</b>	Model	FLT Liquid Turbine Flow Meter
	Measuring range	2-40 $m^3/h$
	Accuracy	0.5%
<b>Pressure Gauge</b>	Type	Analog
	Sensitivity	0.05 bar
<b>Air Compressor</b>	Source	Central compressor (Ingersoll rand)
	Maximum pressure	0.85 MPa
	Maximum flow rate of air	42.5 $m^3 min^{-1}$
<b>Air Flow Meter</b>	Model	Omega FMA-2600A
	Flow range	0-2 $Sm^3/min$
	Accuracy	$\pm 0.05\%$

*Refer to Appendix 2 for more pictures on test rig.*

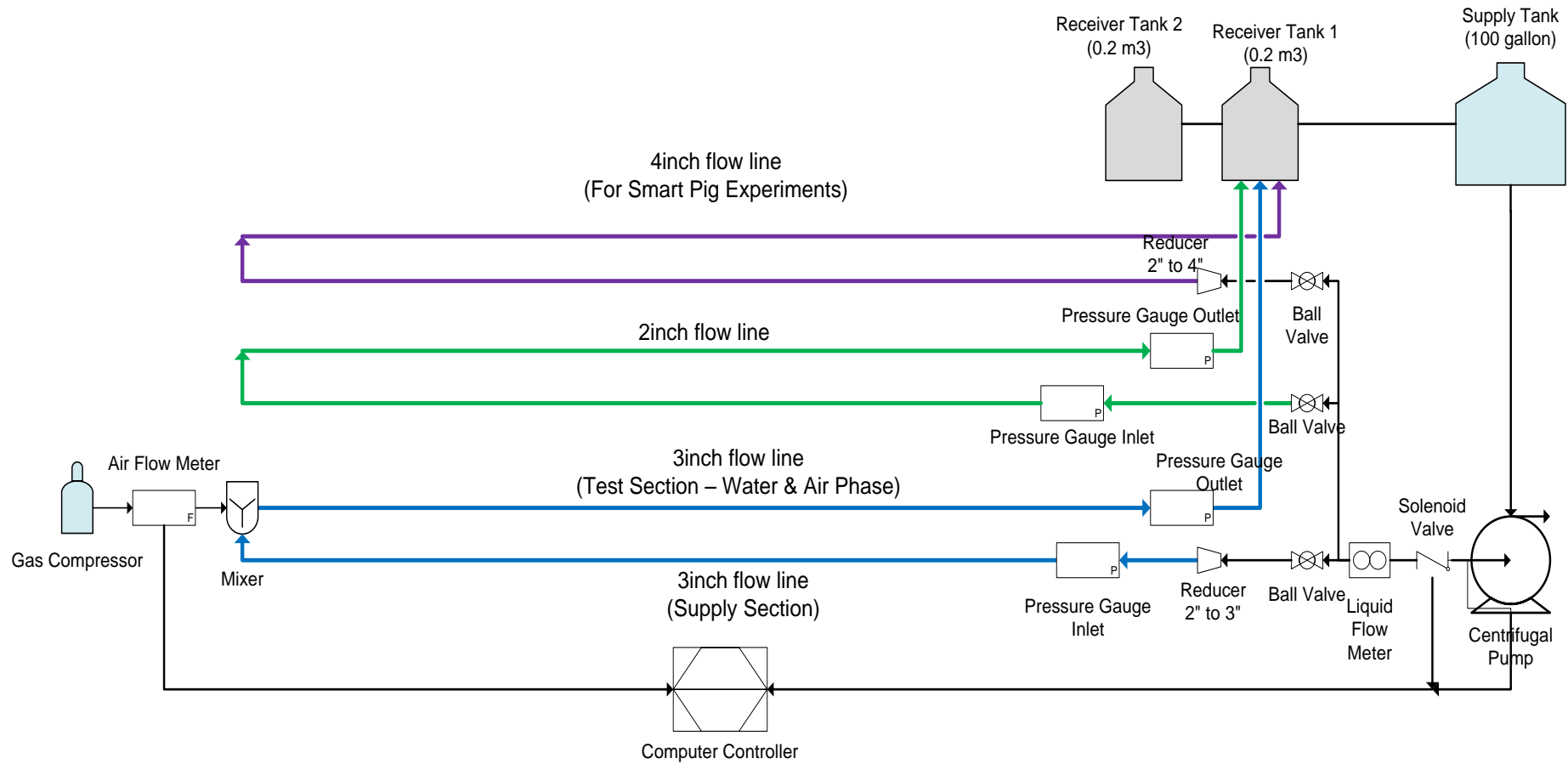


Figure 8: Schematic diagram of integrated three lines flow loop.

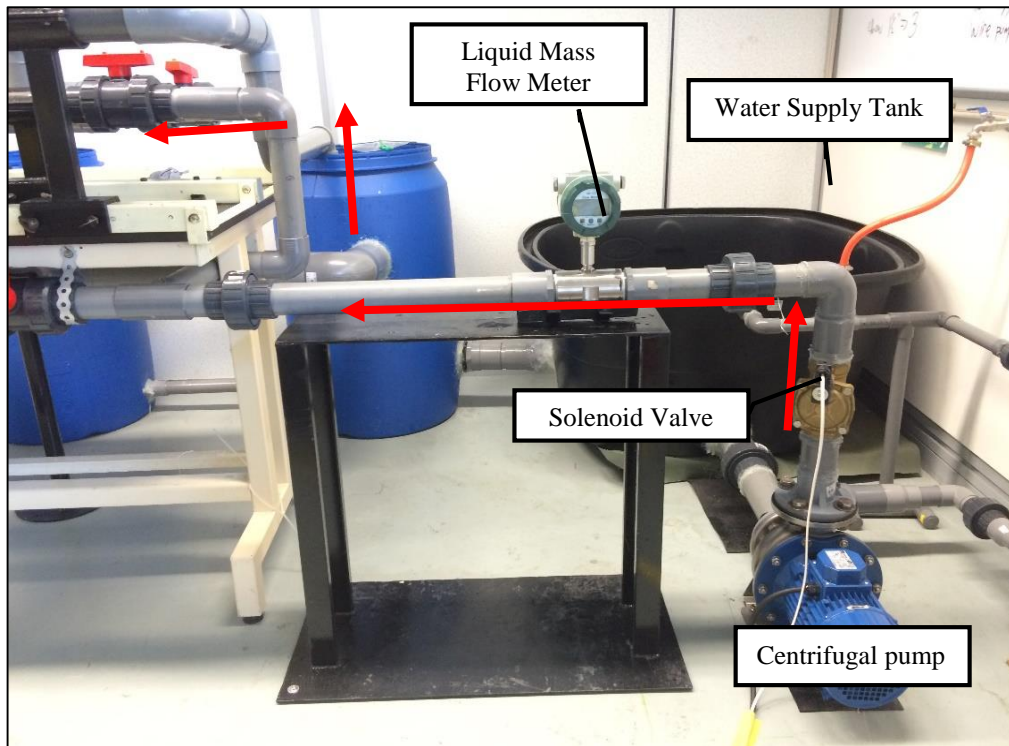


Figure 9: The inlet section of the flow loop, the storage tank, pump, solenoid valve and mass flow meter.

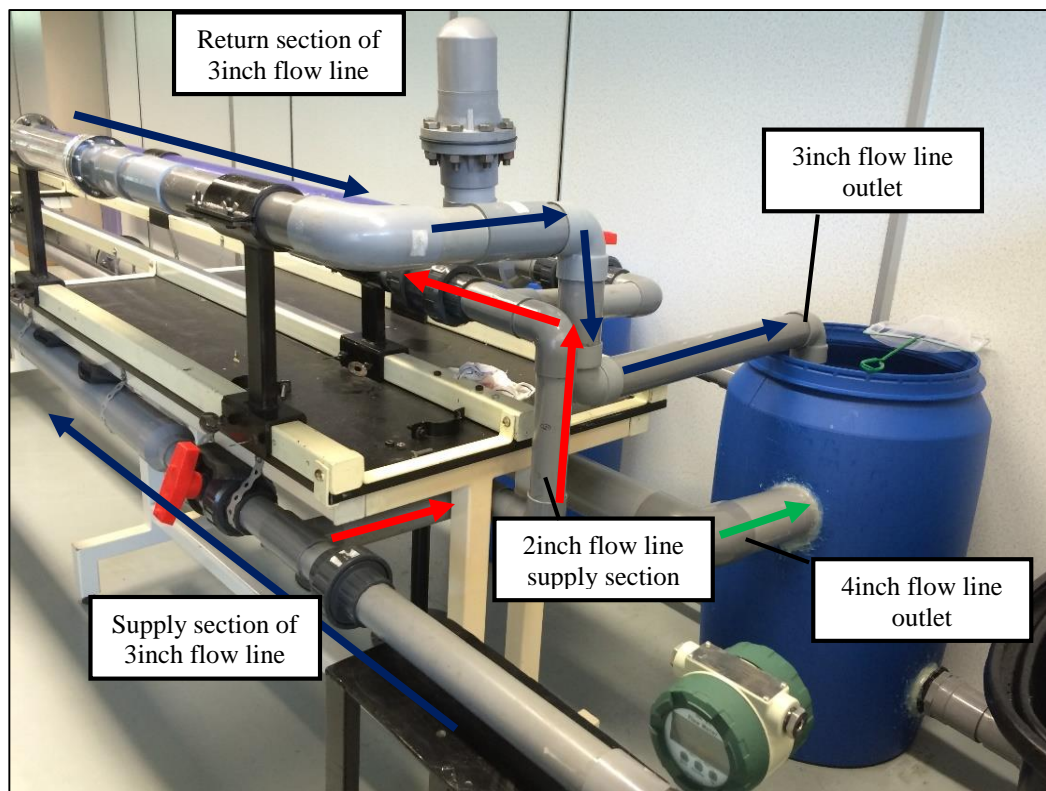


Figure 10: The connection of the flow loop at the inlet where the flow branched into three lines.



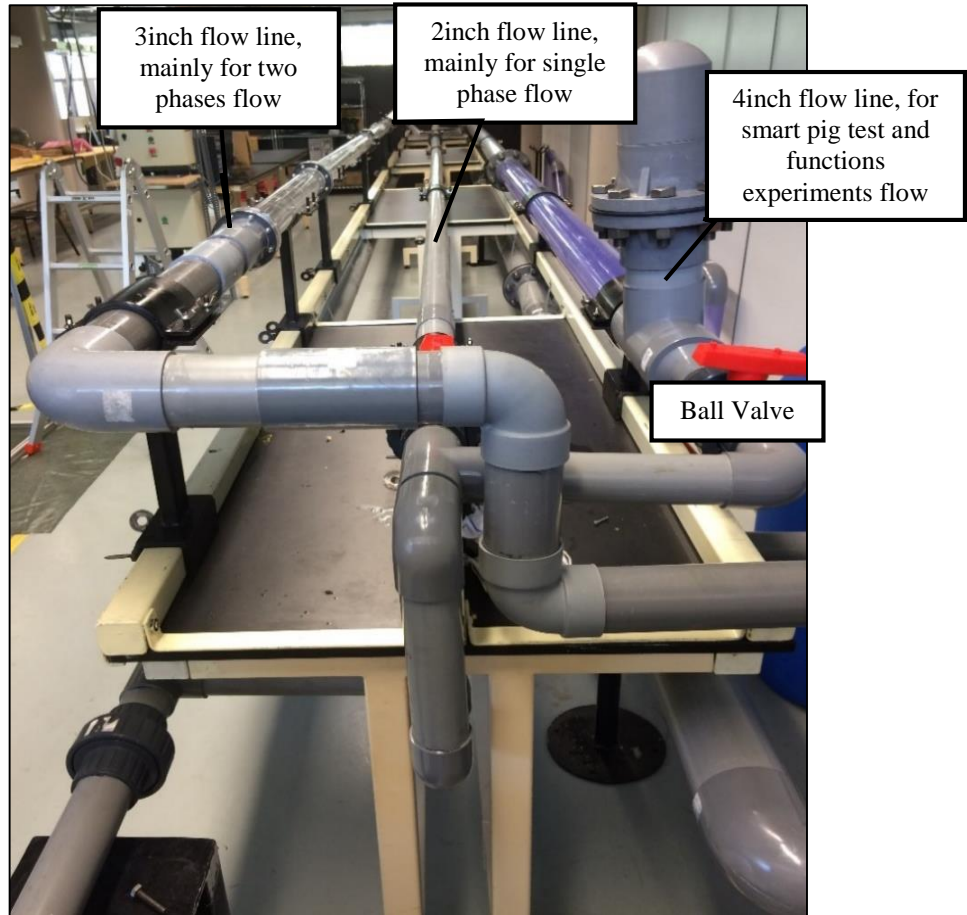


Figure 11: From the left, 3inch, 2inch and 4inch flow line, each flow line has total length of 24m.

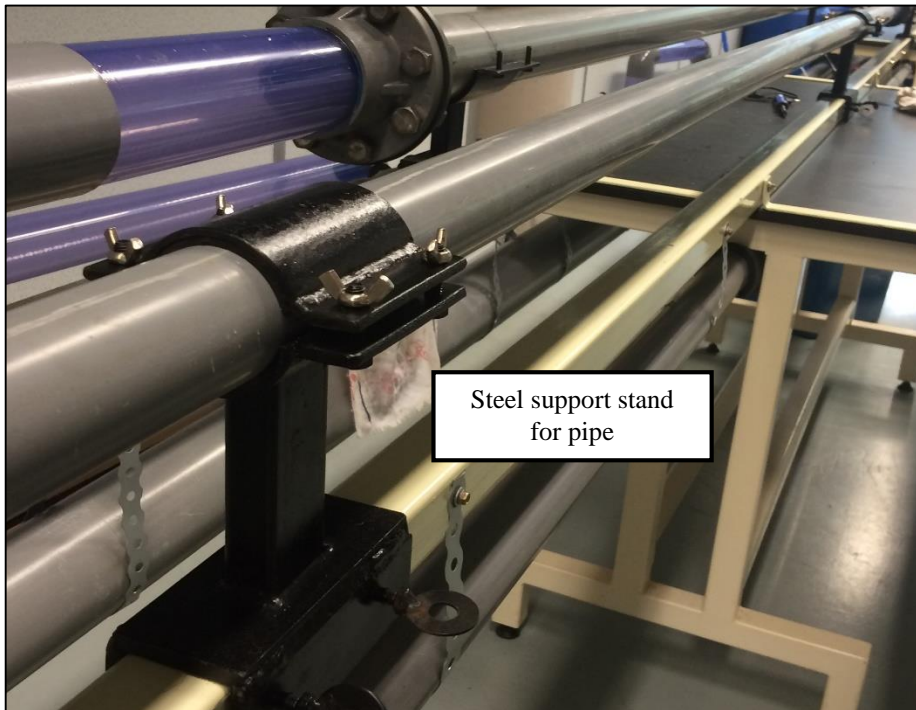


Figure 12: Steel support stand for pipe.



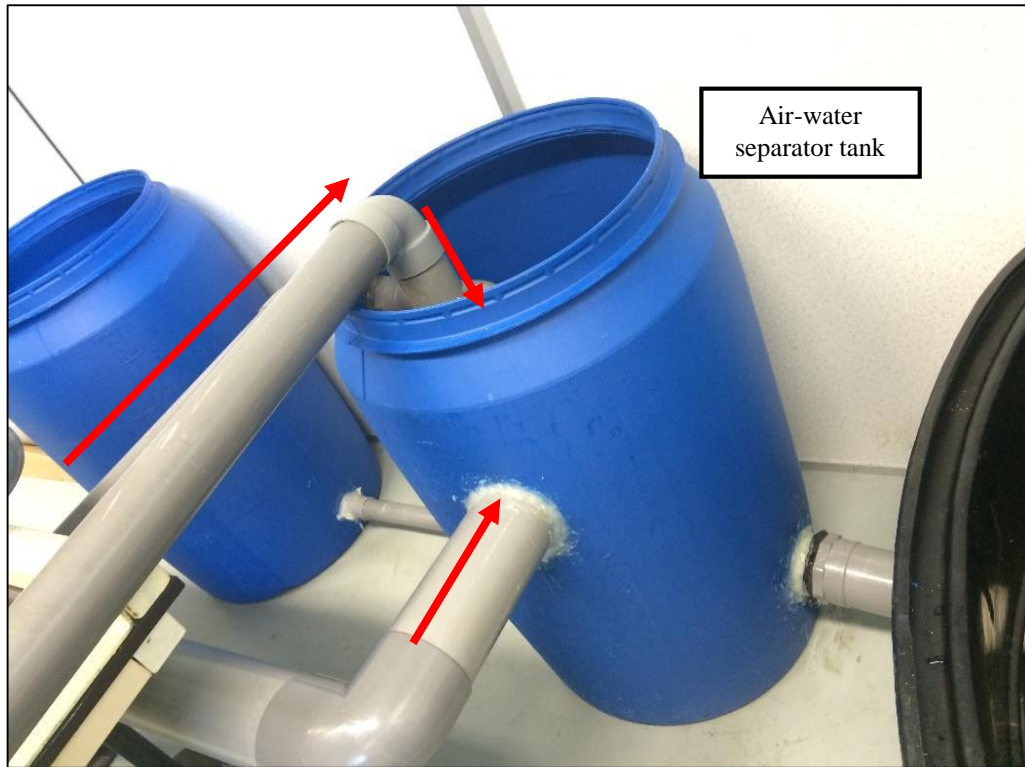


Figure 13: Receiver tanks connection.

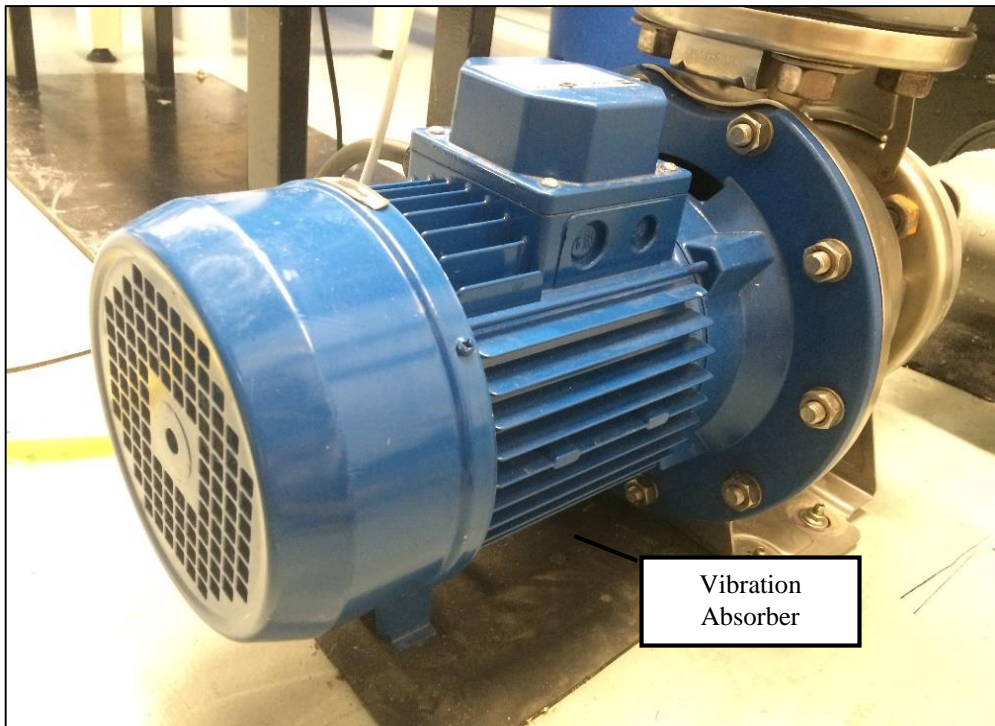


Figure 14: The pump was anchored to ground and a rubber pad was beneath the pump to absorb vibration.

#### **4.1.1 2inch, 3inch and 4inch Flow Line**

The three line flow loop system consists of 2inch flow line, 3inch flow line and 4inch flow line. All the three 2inch, 3inch and 4inch ID flow lines has total length of 24m. All these pipes were clamped on steel structures support to provide sufficient support and avoid vigorous vibration during experiment as shown in Figure 12.

The 2inch flow line is a single phase flow, which only carry water. Class D PVC pipe was connected for the entrance loop which has length of 12m whereas the rest of the 12m was connected by using Class O PVC. Class D PVC pipe at the entrance loop was designed so that to maintain the high pressure in the system. Figure 21 shows the schematic diagram of 2inch flow line.

On the other hand, the 3inch flow line is a two-phase flow system, which are water and air. A mixer was customized-designed by using an elongated plate in the middle to separate the air and water. This also solved the difficulties that may occur at the inlet of two-phase flow test section and to enhance the stratification level at the pipe inlet. Before the inlet of the mixer, the pipe material is Class O PVC. After the mixer, Plexiglas was connected for the return loop. Plexiglas is a transparent material which allows observation to take place. Figure 22 shows the 3inch flow line setup.

The 4inch flow line is used to study the capability of a pigging ball on performing its defined functions. It was made up of two type of material of pipe, they are Class O PVC pipe and transparent PVC pipe. The transparent PVC pipe enable observation purposes. It is not fully made up of transparent PVC due to its high cost. The state of art for the 4inch flow line is that the last 2m at the entrance loop was allowed to interchange with three different configurations of pipes which are the loop with 0°, 45° and 90° inclination. Figures 23-25 shows the different configuration of the 4inch flow line.

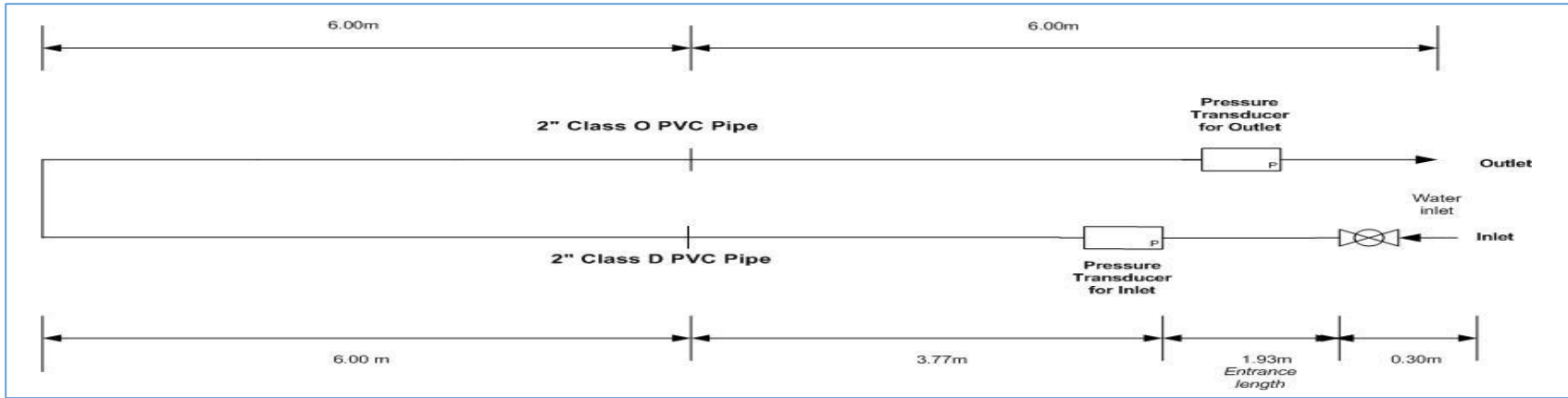


Figure 15: 2inch flow line.

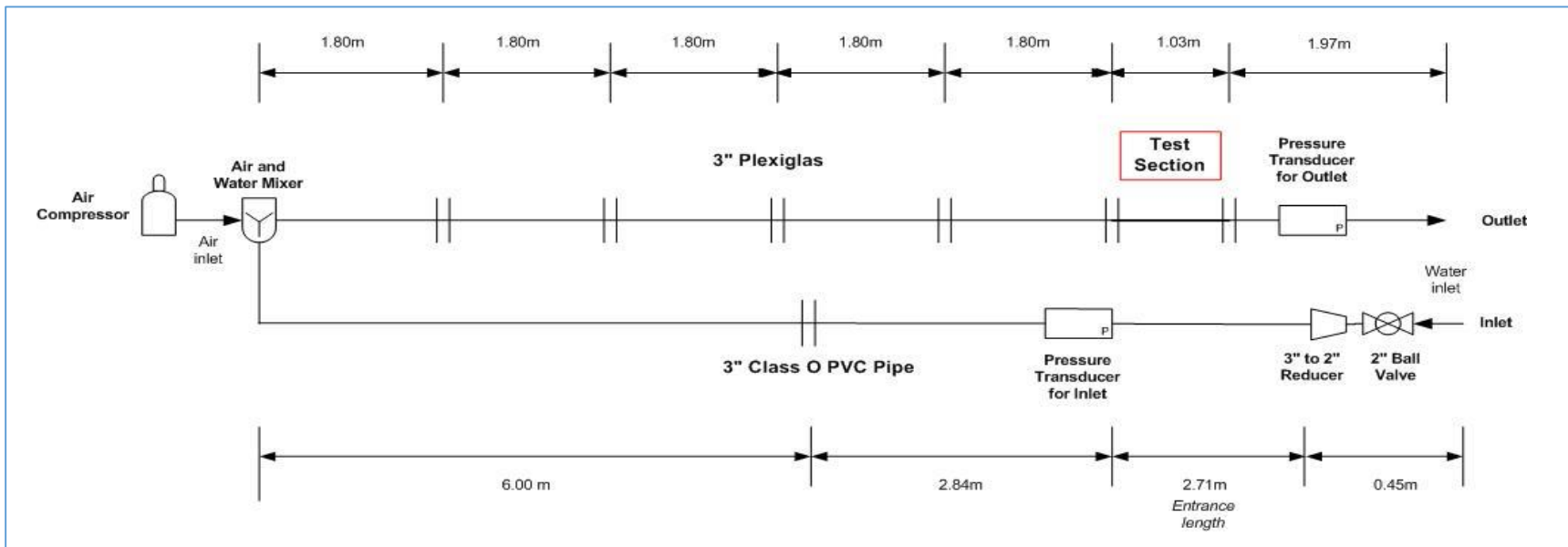


Figure 16: 3inch flow line.

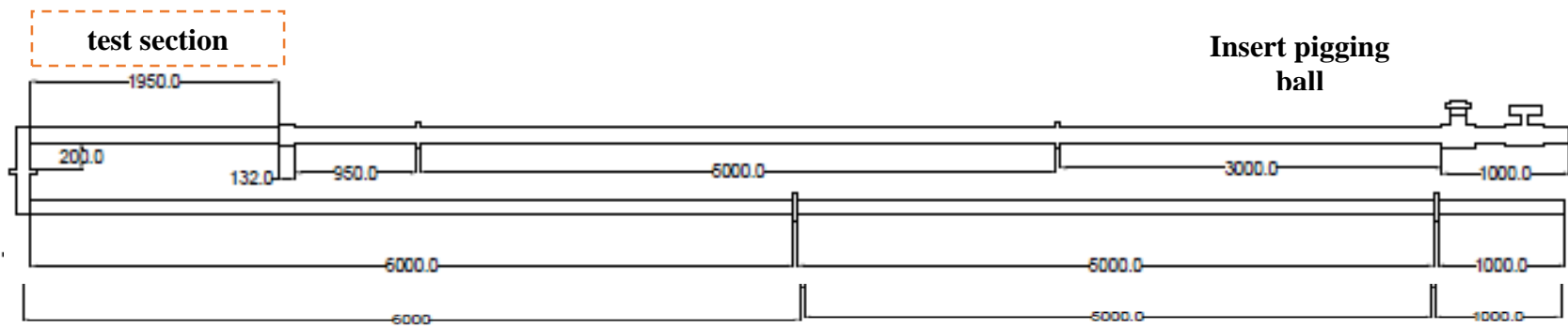


Figure 17: 4inch flow line with 0 degree inclination.

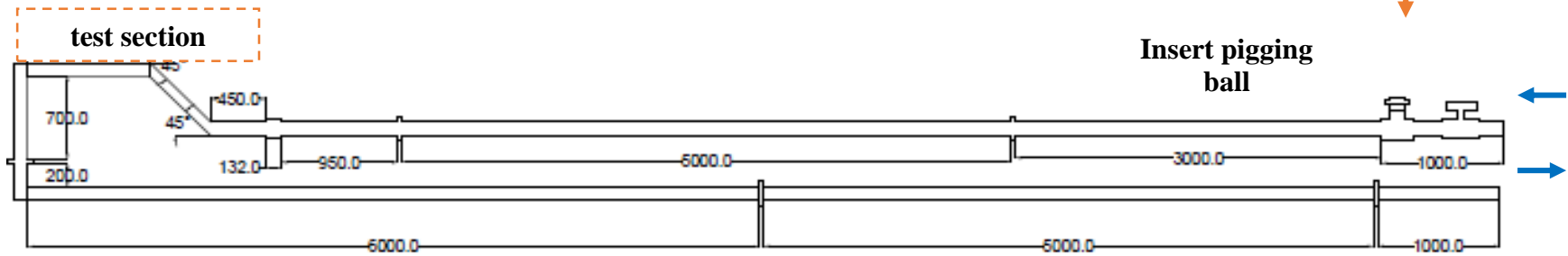


Figure 18: 4inch flow

line with 45 degree inclination.

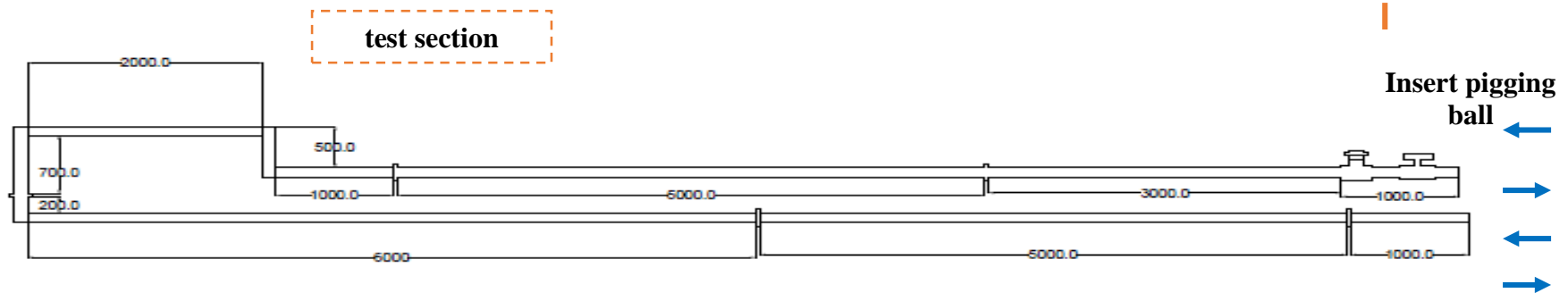


Figure 19: 4inch flow line with 90 degree inclination.



### 4.1.2 Installation of Pressure Gauge

As this experimental require justification on differential pressure of each flow line, hence each flow line was installed with pressure gauge at the inlet as well as the outlet. In order to ensure pressure gauges give accurate readings, the pressure gauges that read the pressure inlet were mounted after the entrance length. This is because after the entrance length, the fluid flow pattern in the pipe is expected to be fully developed. Pressure gauges would then able to read the pressure reading at the fully developed and is more stable. The entrance length of each flow line is determined and tabulated in Table 6.

Table 7: Calculation on entrance length of respective flow line.

Step 1: Determine the centrifugal pump flow rate.	
Considered the maximum pump flow rate which is $60 \text{ m}^3\text{h}^{-1} = 0.0167 \text{ m}^3\text{s}^{-1}$ .	
Step 2: Compute the diameter in meter (m) and crossed-section area.	
<b>2inch Flow line</b>	<b>3inch Flow Line</b>
$D_2 = 0.0508\text{m}$ $A_2 = 2.0268 \times 10^{-3} \text{ m}^2$	$D_3 = 0.0762\text{m}$ $A_3 = 4.560 \times 10^{-3} \text{ m}^2$
Step 3: Calculate the velocity, $v$ at respective flow line. $v = \frac{Q}{A}$	
$v = \frac{0.0167}{2.0268 \times 10^{-3}} = 8.234 \text{ m/s}$	$v = \frac{0.0167}{4.560 \times 10^{-3}} = 3.662 \text{ m/s}$
Step 4: Calculate the Reynold number, $Re$ . $Re = \frac{\rho v D}{\mu}$ Take dynamic viscosity, $\mu$ @20 °C, which is $1.002 \times 10^{-3} \text{ m}^3\text{h}^{-1}$ , Density of water, $\rho$ @20 °C, which is $1000 \text{ kg/m}^3$ .	
$Re = 1000 \times 8.234 \times 0.0508$ $\div 1.002 \times 10^{-3}$ $\approx 4.2 \times 10^5$  Turbulent Flow	$Re = 1000 \times 3.662 \times 0.0762$ $\div 1.002 \times 10^{-3}$ $\approx 2.8 \times 10^5$  Turbulent Flow
Step 5: Calculate the entrance length, $l_e$ of respective flow line. Since the three flow lines has turbulent flow characteristics, hence $l_e = 4.4 D * Re^{\frac{1}{6}}$ .	
$l_e = 1.934\text{m}$	$l_e = 2.710\text{m}$

## 4.2 Justification on Three Lines Flow Loop System

In this experiment only two flow lines which are the 2inch and 3inch flow lines were justified by comparing the theoretical head losses,  $\Sigma h_{L,cal}$  with experimental head losses,  $\Sigma h_{L,exp}$  values. Meanwhile, the 4inch flow lines was experimentally justified by another FYP candidate where the smart pig was tested in the experiment setup.

### 4.2.1 Experimental Values of Head Losses

The experimental head losses,  $\Sigma h_{L,exp}$  values were obtained by measuring differential pressure, velocity change and elevation difference. The differential pressure readings were obtained from pressure gauges where they were installed at the defined two particular points of inlet and outlet; whereas the elevation differences were measured by using measuring tape. For the velocity readings, they were computed from the FLT Liquid Turbine Flow Meter.

*Refer to Appendix 3 for data recordation.*

If there is no change in cross-section area size, it is assumed that the velocity is remained the same and conserved. The readings of velocity and pressure are varied at different flow rate. By having all these readings,  $\Sigma h_{L,exp}$  were then computed by using energy equation that had presented earlier in chapter 3.2.2.

For 2inch flow line, the  $A$  is constant throughout the pipe, hence the  $v$  is assumed to be constant. The readings of  $Q$ ,  $v$ , and  $z$  were recorded and  $\Sigma h_{L,exp}$  were computed as shown in Table 8.

For 3inch flow line, the  $A$  is reduced after 8.7m, hence there is change in  $v$  and is calculated. The readings of  $Q$ ,  $v$ , and  $z$  were recorded and  $\Sigma h_{L,exp}$  were computed as shown in Table 9.

Table 8: Q, v, P and z readings at the inlet and outlet and computed  $\Sigma h_{L,exp}$  for 2inch flow line.

Computer water speed	Q ( $m^3/h$ )	Q ( $m^3/s$ )	v (m/s)	P <sub>1</sub> (kPa)	P <sub>2</sub> (kPa)	z <sub>1</sub> (m)	z <sub>2</sub> (m)	$\Sigma h_{L,exp}$ (m)
60	15.720	0.004	0.958	15.000	0.000	0.760	1.330	0.909
70	18.890	0.005	1.151	20.000	0.000	0.760	1.330	1.397
80	21.630	0.006	1.318	25.000	0.000	0.760	1.330	1.884
90	23.980	0.007	1.461	35.000	5.000	0.760	1.330	2.372
100	25.100	0.007	1.529	40.000	10.000	0.760	1.330	2.361

Table 9: Q, v, P and z readings at the inlet and outlet and computed  $\Sigma h_{L,exp}$  for 3inch flow line.

Computer water speed	Q ( $m^3/h$ )	Q ( $m^3/s$ )	v <sub>1</sub> (m/s)	v <sub>2</sub> (m/s)	P <sub>1</sub> (kPa)	P <sub>2</sub> (kPa)	z <sub>1</sub> (m)	z <sub>2</sub> (m)	$\Sigma h_{L,exp}$ (m)
60	15.720	0.004	0.958	1.379	15.000	0.000	0.760	1.330	0.909
70	18.890	0.005	1.151	1.657	20.000	0.000	0.760	1.330	1.397
80	21.630	0.006	1.318	1.897	25.000	0.000	0.760	1.330	1.884
90	23.980	0.007	1.461	2.103	35.000	5.000	0.760	1.330	2.372
100	25.100	0.007	1.529	2.202	40.000	10.000	0.760	1.330	2.361

#### 4.2.2 Theoretical Head Losses Calculations

The methodology to calculate  $\Sigma h_{L,cal}$  were presented earlier in Chapter 3. The  $Q$  of the line,  $L$  and  $D$  of the loop were recorded. The  $Q$  readings were recorded from the FLT turbine flow meter whereas the  $L$  of the flow loop was measured. The  $v$ ,  $Re$  and  $f$  were then calculated from the  $Q$  given and then to compute the  $h_{L,major}$ ,  $h_{L,minor}$  and  $\Sigma h_{L,cal}$ . The  $\Sigma h_{L,cal}$  values were different at different flow rate.

Table 10 tabulates the values for  $L$  of the loop,  $D$  of pipe and  $\Sigma K_L$  for 2inch flow line. Table 11 shows the recorded and calculated values in order to compute  $\Sigma h_{L,cal}$  of 2inch flow line at different  $Q$ .

Table 12 tabulates the values for  $L$  of the loop,  $D$  of pipe and  $\Sigma K_L$  for 3inch flow line. Since there is a reduction in area for 3inch flow loop, therefore the  $v$  changes and affected  $Re$ ,  $f$ ,  $h_{L,major}$ ,  $h_{L,minor}$  and  $\Sigma h_{L,cal}$ . Table 13 shows the recorded and calculated values in order to compute total head losses,  $\Sigma h_{L,cal}$  of 3inch flow line at different  $Q$ .

Table 10: Length of the loop, diameter of pipe and loss coefficient,  $\Sigma K_L$  for 2inch loop.

<b>Length of the loop:</b>		<b>21.19m</b>	
<b>Diameter:</b>		<b>0.0508m</b>	
<b>Fittings</b>	<b>Quantity</b>	<b><math>K_L</math></b>	<b><math>\Sigma K_L</math></b>
2inch union	2	0.08	0.16
2inch socket	1	0.08	0.08
2inch elbow	2	0.57	1.14
<b>SUM</b>			<b>1.38</b>

Table 11: Recorded, Q and computed v, Re, f,  $h_{L,major}$ ,  $h_{L,minor}$  and  $\Sigma h_{L,cal}$  for 2inch loop.

<b>Computer water speed</b>	<b>Q (<math>m^3/h</math>)</b>	<b>Q (<math>m^3/s</math>)</b>	<b>v (m/s)</b>	<b>Re</b>	<b>f</b>	<b><math>h_{L,major}</math> (m)</b>	<b><math>h_{L,minor}</math> (m)</b>	<b><math>\Sigma h_{L,cal}</math> (m)</b>
<b>60</b>	11.560	0.003	1.584	80322	0.020	1.075	0.176	1.251
<b>70</b>	14.120	0.004	1.935	98109	0.020	1.554	0.263	1.817
<b>80</b>	17.820	0.005	2.442	123818	0.019	2.392	0.419	2.812
<b>90</b>	19.700	0.005	2.700	136881	0.019	2.884	0.512	3.396
<b>100</b>	21.190	0.006	2.904	147234	0.018	3.304	0.593	3.897



Table 12: Length of the loop, diameter of pipe and loss coefficient,  $\Sigma K_L$  for 3inch supply and test sections.

SUPPLY SECTION			
Length of the loop:		8.70m	
Diameter:		0.0762m	
Fittings	Quantity	$K_L$	$\Sigma K_L$
3inch Flange	1	0.200	0.20
3inch Socket	1	0.080	0.08
SUM			<b>0.28</b>

TEST SECTION			
Length of the loop:		12.00m	
Diameter:		0.0635m	
Fittings	Quantity	$K_L$	$\Sigma K_L$
3inch -2.5inch Reducer	1	0.093	0.09
2.5inch 90 elbow	1	0.540	0.54
2.5inch Tee joint	1	1.080	1.08
2.5inch Socket	1	0.080	0.08
2.5inch union	1	0.080	0.08
2.5inch Flange	7	0.200	1.40
SUM			<b>3.27</b>

Table 13: Recorded, Q and computed v, Re, f,  $h_{L,major}$ ,  $h_{L,minor}$  and  $\Sigma h_{L,cal}$  for 3inch loop.

Computer water speed	Q ( $m^3/s$ )	SUPPLY SECTION					TEST SECTION					$\Sigma h_{L,cal}$ (m)
		v (m/s)	Re	f	$h_{L,major}$ (m)	$h_{L,minor}$ (m)	v (m/s)	Re	f	$h_{L,major}$ (m)	$h_{L,minor}$ (m)	
60	0.004	0.958	72824	0.020	0.107	0.013	1.379	87381	0.020	0.359	0.317	0.796
70	0.005	1.151	87509	0.019	0.149	0.019	1.657	105002	0.019	0.503	0.458	1.129
80	0.006	1.318	100202	0.019	0.192	0.025	1.897	120233	0.019	0.646	0.600	1.462
90	0.007	1.461	111088	0.019	0.231	0.030	2.103	133295	0.018	0.782	0.738	1.781
100	0.007	1.529	116277	0.019	0.252	0.033	2.202	139521	0.018	0.851	0.808	1.944

### 4.2.3 Comparison between Experimental and Theoretically Calculated Values of Head Losses

The relationship between  $\Sigma h_{L,exp}$  and  $\Sigma h_{L,cal}$  against Q for 2inch and 3inch lines were plotted. Figure 20 shows the graph of  $\Sigma h_L$  against Q in 2inch flow line whereas Figure 21 shows the graph of  $\Sigma h_L$  against Q in 3inch flow line. According to Figure 20 and 21, it clearly showed that  $\Sigma h_{L,exp}$  are in good agreement with the predicted values,  $\Sigma h_{L,cal}$ . When the flow rate increase, both the  $\Sigma h_{L,exp}$  and  $\Sigma h_{L,cal}$  are then increase. This is because the  $\Sigma h_L$  is proportionally increasing with square of  $v$ .  $\Sigma h_{L,exp}$  in both 2inch and 3inch lines follow the theoretical expectations. It was also observed that the 2inch flow line has higher magnitude of  $\Sigma h_L$ , this is due to its smaller diameter of pipe.

However, the values of  $\Sigma h_{L,exp}$  were higher than  $\Sigma h_{L,cal}$  which calculated theoretically. This is because the computation of  $\Sigma h_{L,exp}$  were not precise. The maximum deliverable pressure by the centrifugal pump is approximately 1.8bar. Due to the special designed of the three lines flow loop system, there are plenty of bending and fittings at the entrance of the loops. This caused significant drop of pressure. Moreover, analog pressure gauge which has low sensitivity of 0.05bar is not good enough to measure the pressure magnitudes. The pressure gauge is ranged between 0 to 7 bar. Other than this, the assumptions of energy equation were not fulfilled absolutely. This is because when the pump running at low flow rate, there are some small air bubbles in the flow line, which make the system not fully incompressible. This decreases the accuracy of  $\Sigma h_{L,exp}$  computation.

On the other hand, some of the pipe fittings  $K_L$  were uncertain such as pipe socket and flange. This caused the theoretically calculated  $\Sigma h_{L,cal}$  were not exact. Further researches should be done in the flow loop to obtain more precise values.

The percentage error between the  $\Sigma h_{L,exp}$  and  $\Sigma h_{L,cal}$  for both the 2inch and 3inch lines are calculated and graphs are plotted as shown in Figure 22 and 23. Percentage error on  $\Sigma h_L$  for 2inch flow line is between 6-22% whereas the percentage error on  $\Sigma h_L$  for 3inch flow line is between 12-24%.

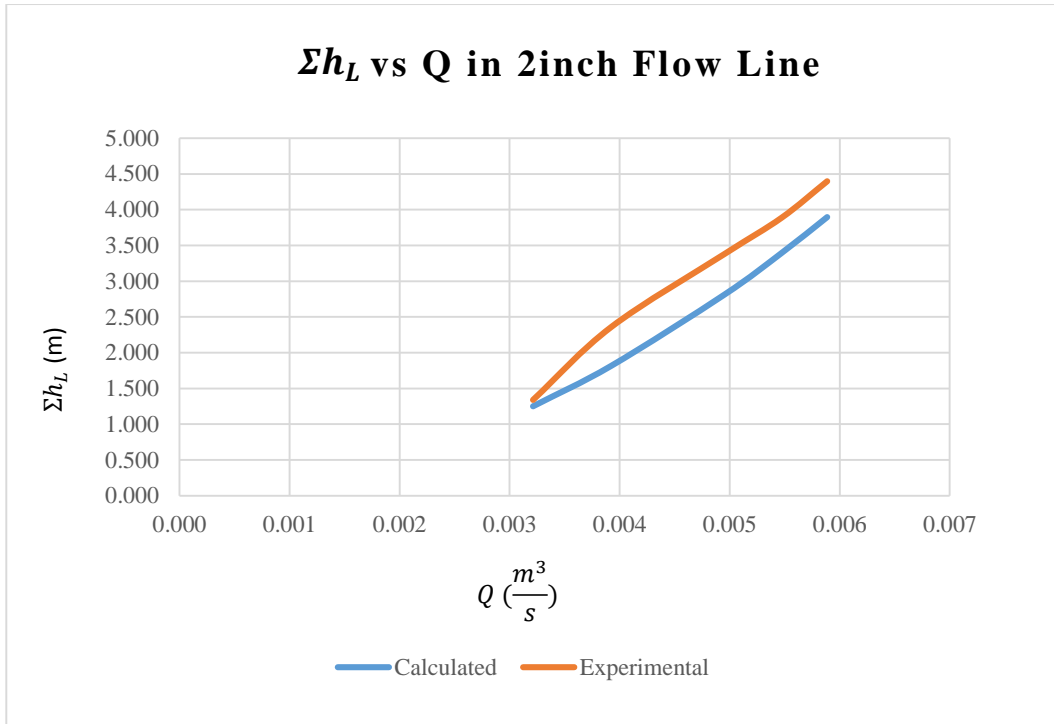


Figure 20:  $\Sigma h_L$  against Q in 2inch flow line.

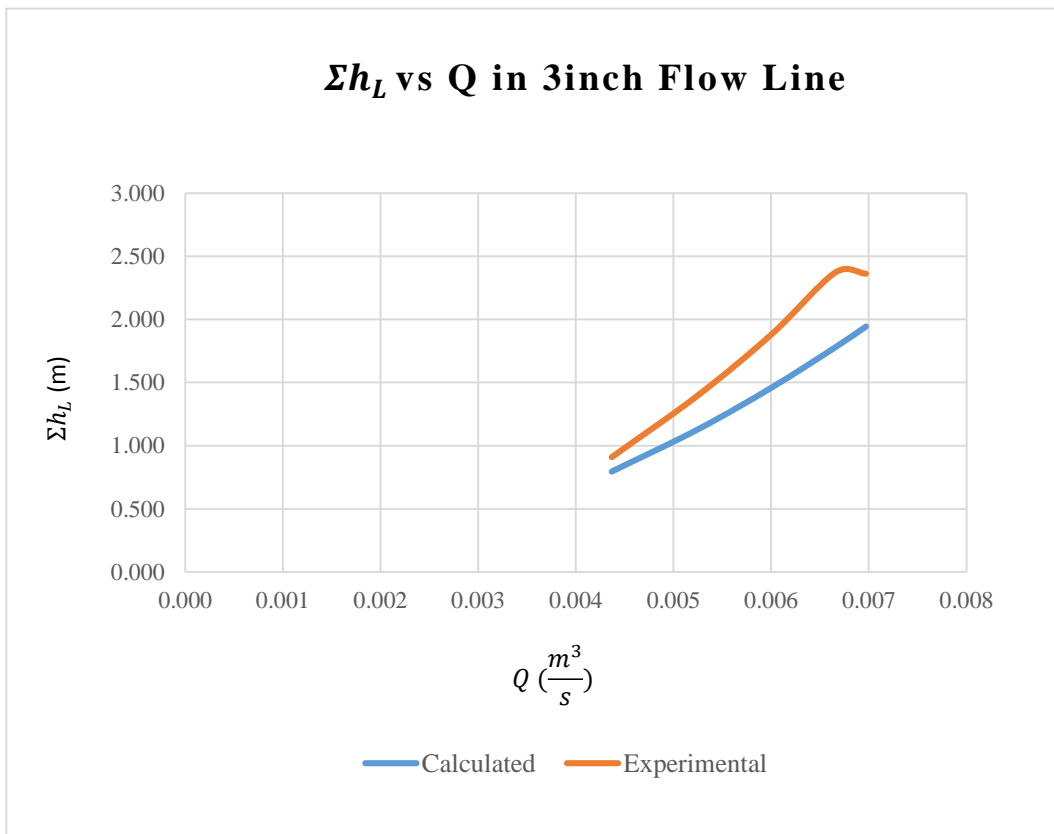


Figure 21:  $\Sigma h_L$  against Q in 3inch flow line.

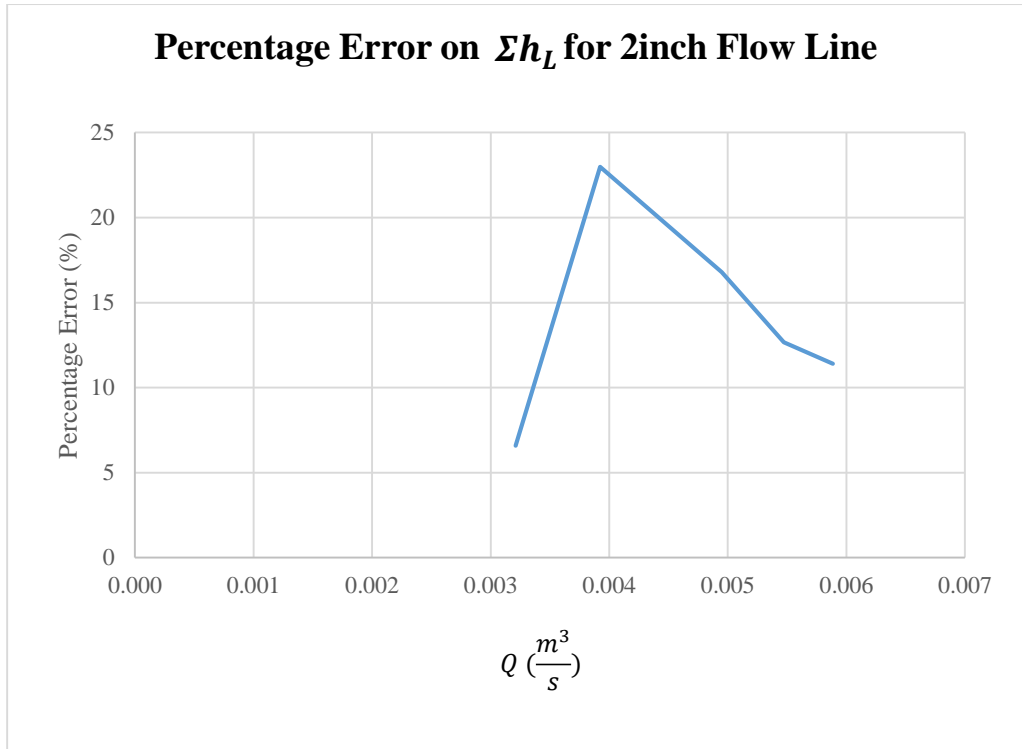


Figure 22: Percentage error on  $\Sigma h_L$  for 2inch flow line.

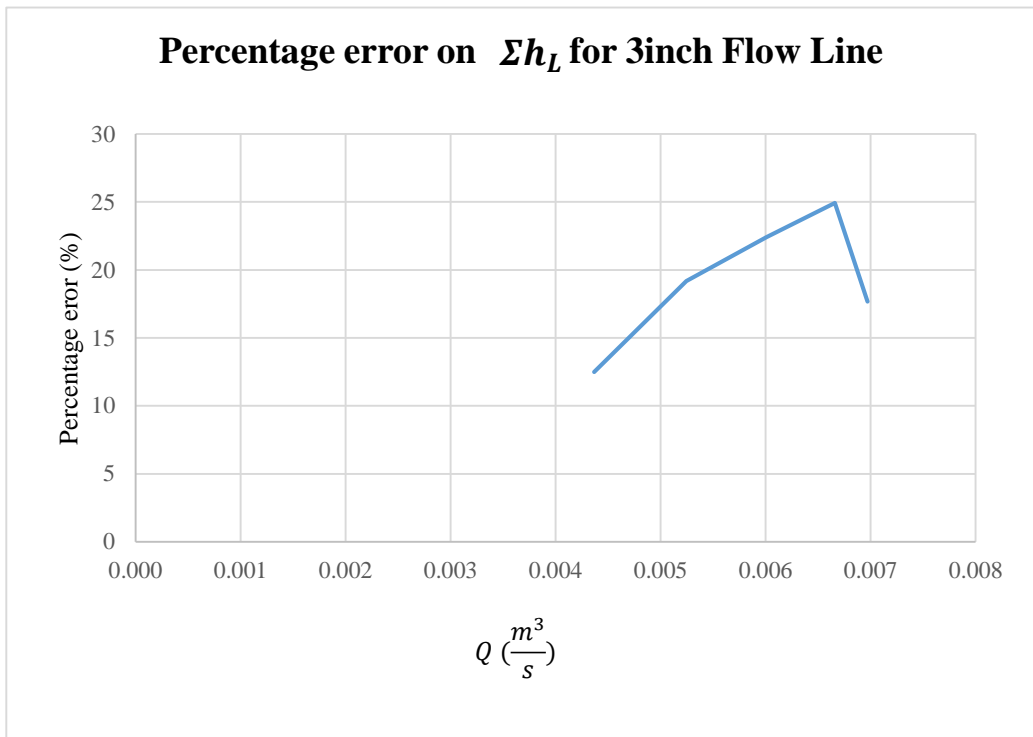


Figure 23: Percentage error on  $\Sigma h_L$  for 3inch flow line.

## CHAPTER 5

### CONCLUSION AND RECOMMENDATION

In the present work, the innovated three lines flow loop test rig was successfully implemented; all the measuring and control devices including centrifugal pump, liquid flow meter, pressure gauge and computer setup were installed correctly. The best part of the test rig is that the three lines are sharing the common centrifugal pump and liquid flow meter. This indeed reduce the cost of implementation and effectively optimize the space of construction indirectly. Besides that, the advanced data acquisition via online control unit enable the users to control the flow rate of pump by using computer. It also allow the users to read the flow rate of air.

Based on the results,  $\Sigma h_{L,exp}$  is in good agreement with the predicted values,  $\Sigma h_{L,cal}$ . A gradual slope change in the head losses is attributed to the change of flow rate. Higher the flow rate, higher the head losses. The difference between  $\Sigma h_{L,exp}$  and  $\Sigma h_{L,cal}$  in the 2inch and 3inch flow lines are considerably acceptable as they are fall below 25 percentage error. In order to improve the experimental setup, it is recommended that the pressure gauge is replaced with digital pressure transducer with good sensitivity e.g.  $\pm 0.01$  bar and the range should be fall within 0-2 bar. This is because of the system is running with low head centrifugal pump. Secondly, more experimental research should be done to study the coefficient loss of uncertain pipe fittings. This is due to the the uncertain  $\Sigma K_L$  in the system, the predicted values might varied the results.

The integrated three lines flow loop system indeed contributes high value to research studies as it has three different sizes of diameter of flow lines and definitely can be used for wide range of research studies in the future.

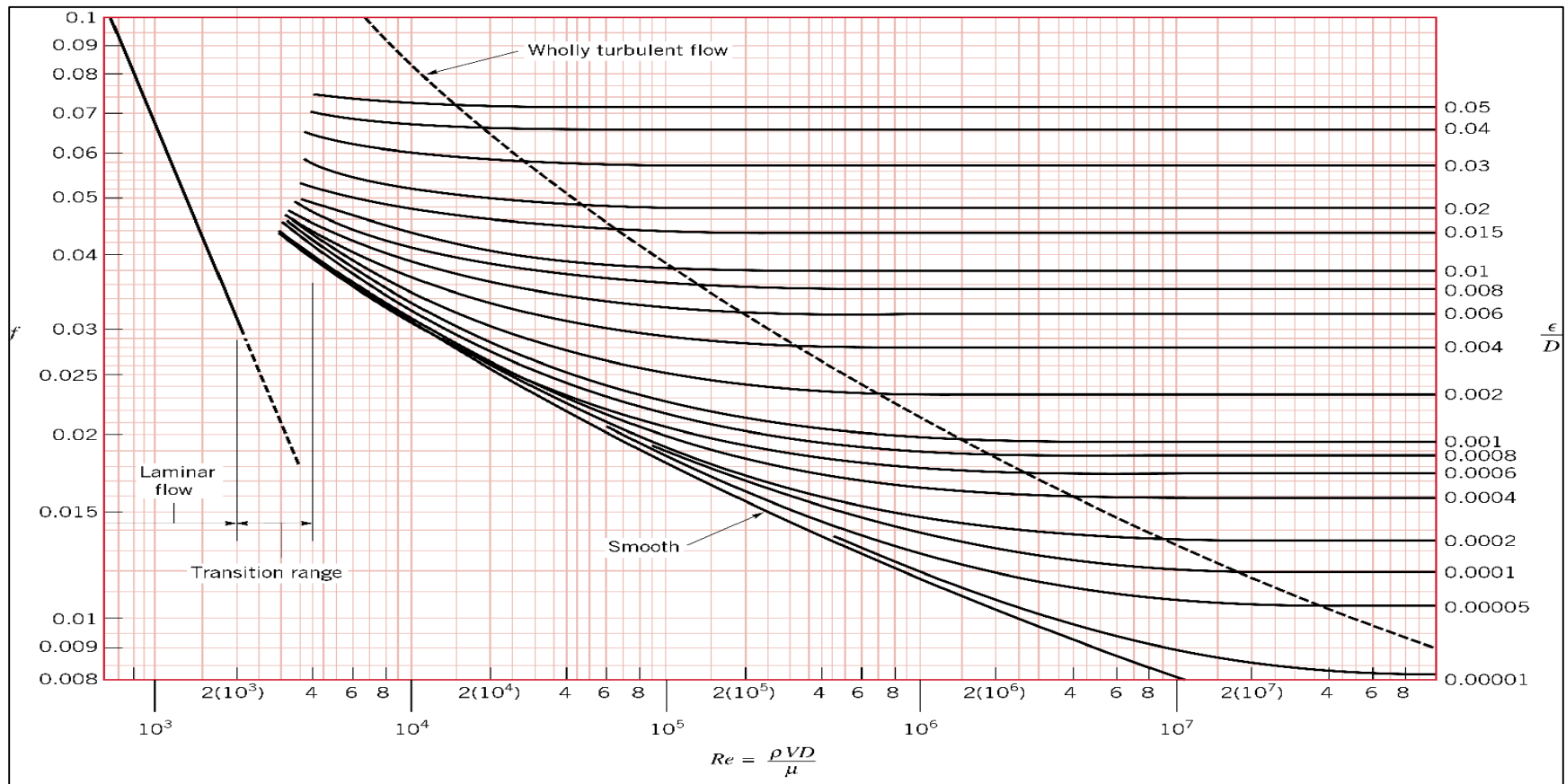
## REFERENCE

- [1] W. M. Abed, R. D. Whalley, D. J. C. Dennis, and R. J. Poole, "Numerical and experimental investigation of heat transfer and fluid flow characteristics in a micro-scale serpentine channel," *International Journal of Heat and Mass Transfer*, vol. 88, pp. 790-802, 2015.
- [2] W. Qu, and I. Mudawar, "Experimental and numerical study of pressure drop and heat transfer in a single-phase micro-channel heat sink," *International Journal of Heat and Mass Transfer*, vol. 45, pp. 2549–2565, 2002.
- [3] X. Tang, X. Dai, and D. Zhu, "Experimental and numerical investigation of convective heat transfer and fluid flow in twisted spiral tube," *International Journal of Heat and Mass Transfer*, vol. 90, pp. 523-541, 2015.
- [4] Z. Xiong, H. Gu, and S. Gong, "Experimental and numerical study on the flow pattern of the ADS windowless spallation target with a second free surface downstream using model fluid water," *Nuclear Engineering and Design*, vol. 291, pp. 179-187, 2015.
- [5] H. Ge, W. Guo, L. Shen, T. Song, and J. Xiao, "Experimental investigation on biomass gasification using chemical looping in a batch reactor and a continuous dual reactor," *Chemical Engineering Journal*, vol. 286, pp. 689-700, 2016.
- [6] F. Liang, Y. Sun, G. Yang, and L. Song, "Gas–liquid two-phase flow rate measurement with a multi-nozzle sampling method," *Experimental Thermal and Fluid Science*, vol. 68, pp. 82-88, 2015.
- [7] M. Wang, J. Jia, Y. Faraj, Q. Wang, C.-g. Xie, G. Oddie, et al., "A new visualisation and measurement technology for water continuous multiphase flows," *Flow Measurement and Instrumentation*, 2015.
- [8] K. E. Kee, M. Babic, S. Richter, L. Paolinelli, W. Li, and S. Nesic, "Flow Patterns and Water Wetting in Gas-Oil-Water Three-phase Flow – A Flow Loop Study," in *NACE Int. Corrosion Conf. and Expo*, 2015.
- [9] X. Lv, B. Shi, Y. Wang, and J. Gong, "Study on Gas Hydrate Formation and Hydrate Slurry Flow in a Multiphase Transportation System," *Energy & Fuels*, vol. 27, pp. 7294-7302, 2013.

- [10] N. Li, L. Guo, and W. Li, "Gas–liquid two-phase flow patterns in a pipeline–riser system with an S-shaped riser," *International Journal of Multiphase Flow*, vol. 55, pp. 1-10, 2013.
- [11] J. Ye and L. Guo, "Multiphase flow pattern recognition in pipeline–riser system by statistical feature clustering of pressure fluctuations," *Chemical Engineering Science*, vol. 102, pp. 486-501, 2013.
- [12] A. Mohmmed, H. H. Al- Kayiem, M. S. Nasif, and Z. Al-Hashimy, "Experimental Investigation on the Slug Flow Characteristics in a Horizontal Pipe", 2015.
- [13] D. Wu, B. Yang, and Y. Liu, "Pressure drop in loop pipe flow of fresh cemented coal gangue–fly ash slurry: Experiment and simulation," *Advanced Powder Technology*, vol. 26, pp. 920-927, 2015.
- [14] B. R. Munson, D. F. Young, T. H. Okiishi, and W. W. Huebsch, *Fundamental of Fluid Mechanics*, 6th ed., John Wiley & Sons, Inc., 2010.
- [15] R. L. Mott, *Applied Fluid Mechanics*, 6<sup>th</sup> ed. Pearson Prentice Hall, 2006.
- [16] *Pipe Flow Expert 2016*. United Kingdom: Pipe Flow, 2016.

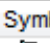
















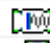











# APPENDIX

## Appendix 1: Head Losses Calculation































Appendix 1.1: Moody chart

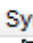
















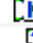





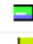







Symbol 	Type	Metric	Imperial	Description	K
	SB	50 mm	2"	Standard Bend	0.5700
	LB	50 mm	2"	Long Bend	0.3000
	PB	50 mm	2"	Pipe Bend	0.2300
	E45	50 mm	2"	Elbow 45 deg.	0.3000
	RB	50 mm	2"	Return Bend	0.9500
	MB45	50 mm	2"	Mitre Bend 45 deg.	0.2900
	MB90	50 mm	2"	Mitre Bend 90 deg.	1.1400
	Gate	50 mm	2"	Gate Valve	0.1500
	Globe	50 mm	2"	Globe Valve	6.5000
	Angle	50 mm	2"	Globe Valve Angled	2.8500
	Plug	50 mm	2"	Plug Valve Straightway	0.3400
	Bfly	50 mm	2"	Butterfly Valve	0.8600
	BallFB	50 mm	2"	Ball Valve Full Bore	0.0600
	BallRB	50 mm	2"	Ball Valve Reduced Bore	1.8000
	LiftCh	50 mm	2"	Lift Check Valve	11.4000
	AngleCh	50 mm	2"	Lift Check Valve Angled	1.1000
	SwCh	50 mm	2"	Swing Check Valve	2.4000
	TiltCh	50 mm	2"	Tilting Disk Check	2.3000
	ChWaf	50 mm	2"	Wafer Check Valve	8.4000
	Foot	50 mm	2"	Foot Valve with Strainer	8.0000
	Hinged	50 mm	2"	Hinged Foot Valve with Strainer	1.4000
	St	50 mm	2"	Strainer	1.0000
	TT	50 mm	2"	Through Tee	0.3800
	BT	50 mm	2"	Branch Tee	1.1400
	ExitCon	50 mm	2"	Pipe Exit to Container	1.0000
	Open	50 mm	2"	Open Pipe Exit	1.0000
	EntProj	50 mm	2"	Pipe Entry Projecting	0.7800
	EntSharp	50 mm	2"	Pipe Entry Sharp	0.5000

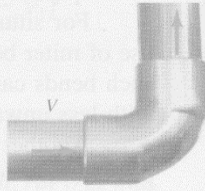
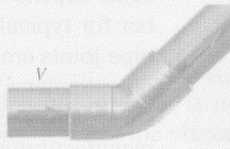
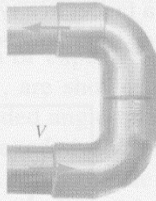
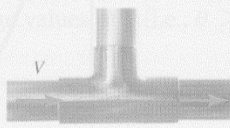
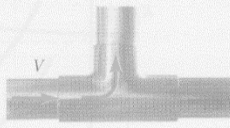

Appendix 1.2:  $K_L$  of 2inch fittings.

Symbol $\frac{A}{Z}$	Type $\frac{A}{Z}$	Metric $\frac{A}{Z}$	Imperial $\frac{A}{Z}$	Description $\frac{A}{Z}$	K $\frac{A}{Z}$
	SB	65 mm	2-1/2"	Standard Bend	0.5400
	LB	65 mm	2-1/2"	Long Bend	0.2900
	PB	65 mm	2-1/2"	Pipe Bend	0.2200
	E45	65 mm	2-1/2"	Elbow 45 deg.	0.2900
	RB	65 mm	2-1/2"	Return Bend	0.9000
	MB45	65 mm	2-1/2"	Mitre Bend 45 deg.	0.2700
	MB90	65 mm	2-1/2"	Mitre Bend 90 deg.	1.0800
	Gate	65 mm	2-1/2"	Gate Valve	0.1400
	Globe	65 mm	2-1/2"	Globe Valve	6.1000
	Angle	65 mm	2-1/2"	Globe Valve Angled	2.7000
	Plug	65 mm	2-1/2"	Plug Valve Straightway	0.3200
	Bfly	65 mm	2-1/2"	Butterfly Valve	0.8100
	BallFB	65 mm	2-1/2"	Ball Valve Full Bore	0.0500
	BallRB	65 mm	2-1/2"	Ball Valve Reduced Bore	1.5000
	LiftCh	65 mm	2-1/2"	Lift Check Valve	10.8000
	AngleCh	65 mm	2-1/2"	Lift Check Valve Angled	1.0000
	SwCh	65 mm	2-1/2"	Swing Check Valve	2.3000
	TiltCh	65 mm	2-1/2"	Tilting Disk Check	2.2000
	ChWaf	65 mm	2-1/2"	Wafer Check Valve	7.0800
	Foot	65 mm	2-1/2"	Foot Valve with Strainer	7.6000
	Hinged	65 mm	2-1/2"	Hinged Foot Valve with Strainer	1.4000
	St	65 mm	2-1/2"	Strainer	1.0000
	TT	65 mm	2-1/2"	Through Tee	0.3600
	BT	65 mm	2-1/2"	Branch Tee	1.0800
	ExitCon	65 mm	2-1/2"	Pipe Exit to Container	1.0000
	Open	65 mm	2-1/2"	Open Pipe Exit	1.0000
	EntProj	65 mm	2-1/2"	Pipe Entry Projecting	0.7800
	EntSharp	65 mm	2-1/2"	Pipe Entry Sharp	0.5000

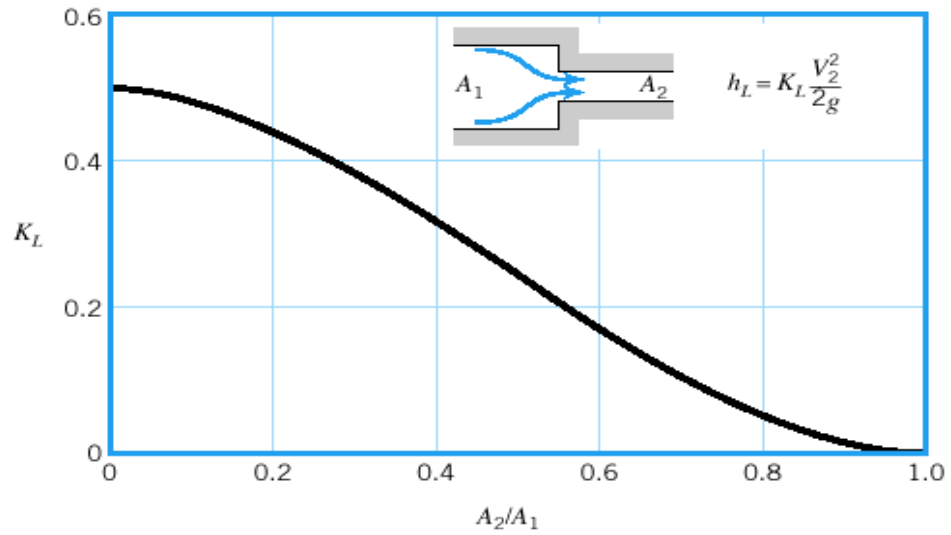
Appendix 1.3:  $K_L$  of 2-1/2inch fittings.

Symbol 	Type	Metric	Imperial	Description	K
	SB	80 mm	3"	Standard Bend	0.5300
	LB	80 mm	3"	Long Bend	0.2800
	PB	80 mm	3"	Pipe Bend	0.2100
	E45	80 mm	3"	Elbow 45 deg.	0.2800
	RB	80 mm	3"	Return Bend	0.8900
	MB45	80 mm	3"	Mitre Bend 45 deg.	0.2700
	MB90	80 mm	3"	Mitre Bend 90 deg.	1.0600
	Gate	80 mm	3"	Gate Valve	0.1400
	Globe	80 mm	3"	Globe Valve	6.0000
	Angle	80 mm	3"	Globe Valve Angled	2.6500
	Plug	80 mm	3"	Plug Valve Straightway	0.3200
	Bfly	80 mm	3"	Butterfly Valve	0.8100
	BallFB	80 mm	3"	Ball Valve Full Bore	0.0500
	BallRB	80 mm	3"	Ball Valve Reduced Bore	1.2000
	LiftCh	80 mm	3"	Lift Check Valve	10.8000
	AngleCh	80 mm	3"	Lift Check Valve Angled	1.0000
	SwCh	80 mm	3"	Swing Check Valve	2.2000
	TiltCh	80 mm	3"	Tilting Disk Check	2.2000
	ChWaf	80 mm	3"	Wafer Check Valve	5.5000
	Foot	80 mm	3"	Foot Valve with Strainer	7.6000
	Hinged	80 mm	3"	Hinged Foot Valve with Strainer	1.4000
	St	80 mm	3"	Strainer	1.0000
	TT	80 mm	3"	Through Tee	0.3600
	BT	80 mm	3"	Branch Tee	1.0800
	ExitCon	80 mm	3"	Pipe Exit to Container	1.0000
	Open	80 mm	3"	Open Pipe Exit	1.0000
	EntProj	80 mm	3"	Pipe Entry Projecting	0.7800
	EntSharp	80 mm	3"	Pipe Entry Sharp	0.5000

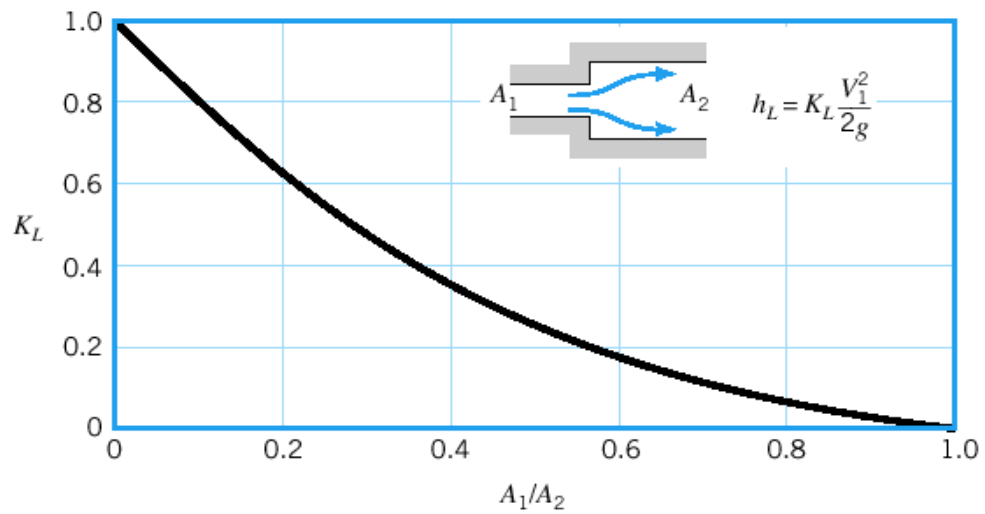
Appendix 1.4:  $K_L$  of 4inch fittings.

Component	$K_L$	
<b>a. Elbows</b>		
Regular 90°, flanged	0.3	
Regular 90°, threaded	1.5	
Long radius 90°, flanged	0.2	
Long radius 90°, threaded	0.7	
Long radius 45°, flanged	0.2	
Regular 45°, threaded	0.4	
<b>b. 180° return bends</b>		
180° return bend, flanged	0.2	
180° return bend, threaded	1.5	
<b>c. Tees</b>		
Line flow, flanged	0.2	
Line flow, threaded	0.9	
Branch flow, flanged	1.0	
Branch flow, threaded	2.0	
<b>d. Union, threaded</b>		
	0.08	
<b>*e. Valves</b>		
Globe, fully open	10	
Angle, fully open	2	
Gate, fully open	0.15	
Gate, $\frac{1}{4}$ closed	0.26	
Gate, $\frac{1}{2}$ closed	2.1	
Gate, $\frac{3}{4}$ closed	17	
Swing check, forward flow	2	
Swing check, backward flow	$\infty$	
Ball valve, fully open	0.05	
Ball valve, $\frac{1}{3}$ closed	5.5	
Ball valve, $\frac{2}{3}$ closed	210	

Appendix 1.5:  $K_L$  of pipe components.



Appendix 1.6: Loss coefficient of sudden contraction.

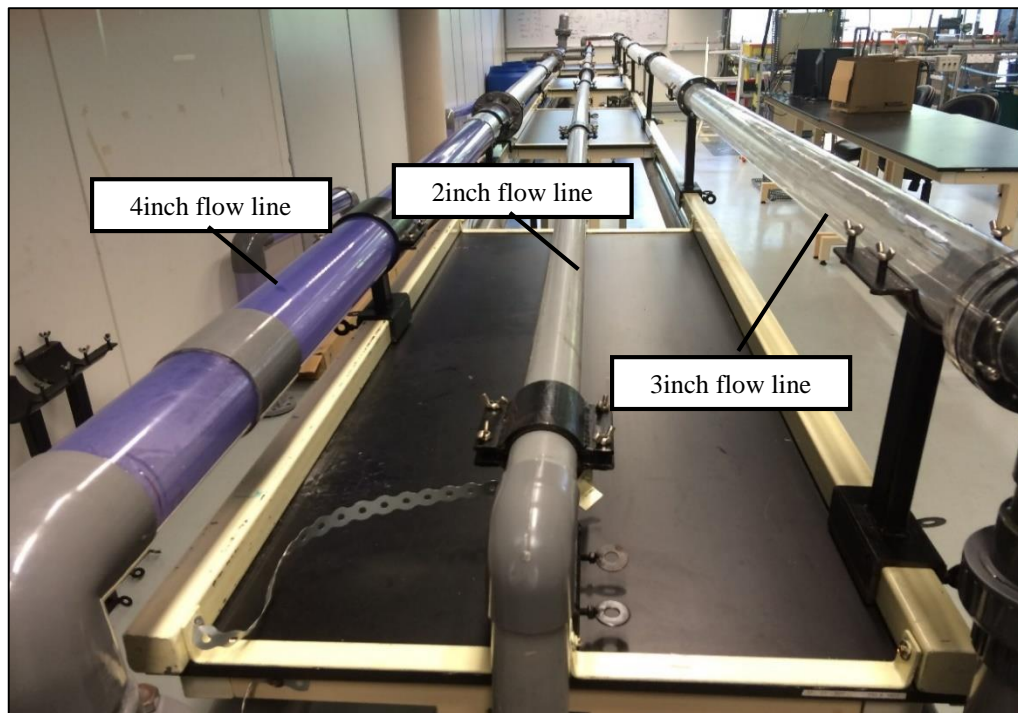


Appendix 1.7: Loss coefficient of sudden expansion.

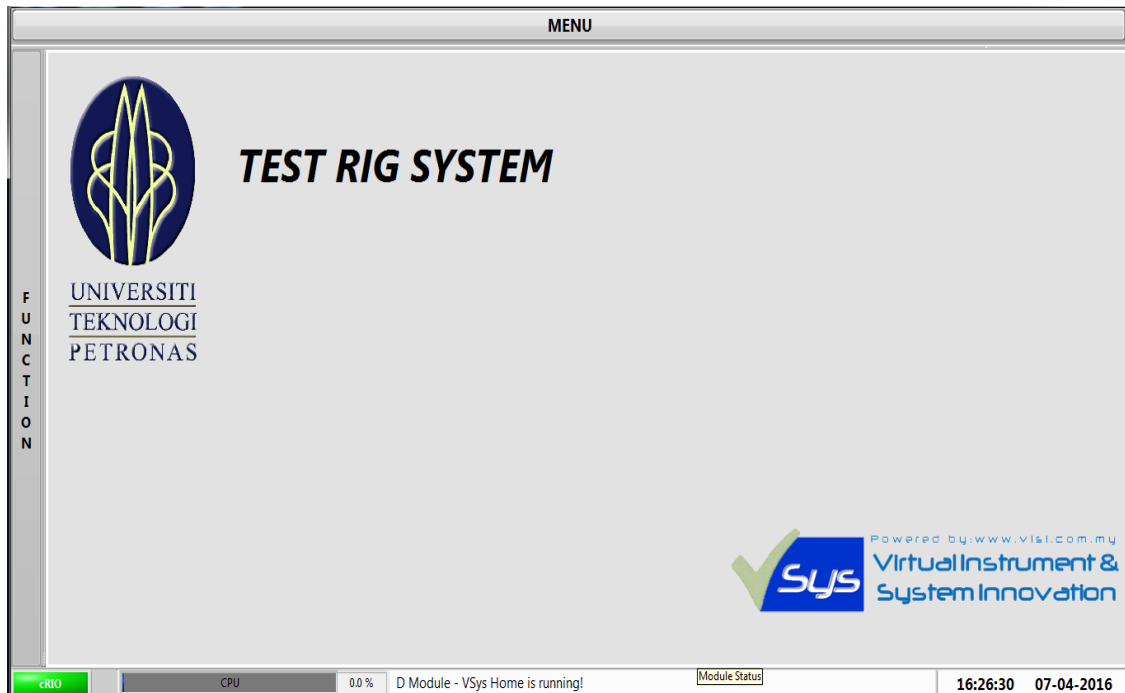
**Appendix 2: Three Lines Flow Loop Setup**



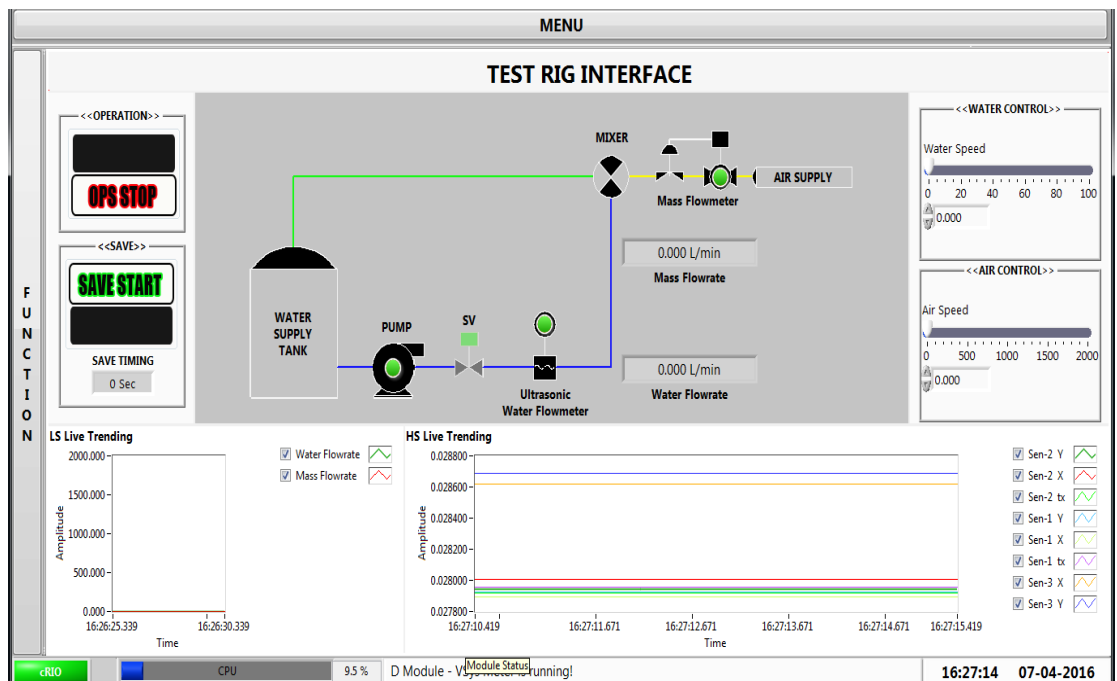
Appendix 2.1: The supply water tank and the water inlet source.



Appendix 2.2: The 12m long flow lines view.



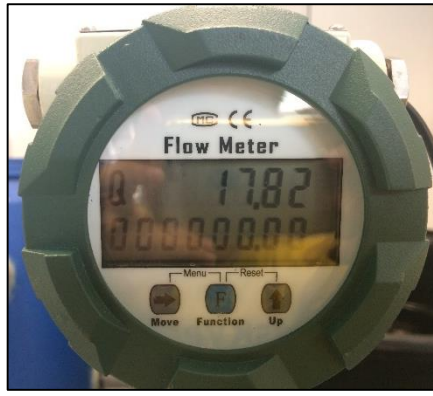
Appendix 2.3: The home page of computer control panel, Test Rig System.



Appendix 2.4: The operation control page of Test Rig System.



### Appendix 3: Data Recording



Appendix 3.1: Flow rate of 2inch flow line at computer water speed of 80.



Appendix 3.2: Inlet pressure of 2inch flow line at computer water speed of 80.



Appendix 3.3: Outlet pressure of 2inch flow line at computer water speed of 80.